Apoptosis-detecting radioligands: current state of the art and future perspectives

Christophe M. M. Lahorte[1], Jean-Luc Vanderheyden[2], Neil Steinmetz[2], Christophe Van de Wiele[3], Rudi A. Dierckx[3], Guido Slegers[1]

[1] Department of Radiopharmacy, Faculty of Pharmaceutical Sciences, Ghent University, Ghent, Belgium
[2] Division of North American Scientific Inc., Theseus Imaging Corporation, Boston, MA, USA
[3] Department of Nuclear Medicine, Ghent University Hospital, Ghent, Belgium

Published online: 12 May 2004

Abstract. This review provides a critical and thorough overview of the radiopharmaceutical development and in vivo evaluation of all apoptosis-detecting radioligands that have emerged so far, along with their possible applications in nuclear medicine. The following SPECT and PET radioligands are discussed: all forms of halogenated Annexin V (i.e. ^{123}I-labelled, ^{124}I-labelled, ^{125}I-labelled, ^{18}F-labelled), ^{99m}Tc/^{94m}Tc-labelled Annexin V derivatives using different chelators and co-ligands (i.e. BTAP, Hynic, iminothiolane, MAG_3, EDDA, EC, tricarbonyl, SDH) or direct ^{99m}Tc-labelling, ^{99m}Tc-labelled Annexin V mutants and ^{99m}Tc/^{18}F-radiopeptide constructs (i.e. AFIM molecules), ^{111}In-DTPA-PEG-Annexin V, ^{11}C-Annexin V and ^{64}Cu-, ^{67}Ga- and ^{68}Ga-DOTA-Annexin V. In addition, the potential role and clinical relevance of anti-PS monoclonal antibodies and other alternative apoptosis markers are reviewed, including: anti-Annexin V monoclonal antibodies, radiolabelled caspase inhibitors and substrates and mitochondrial membrane permeability targeting radioligands. Nevertheless, major emphasis is placed on the group of Annexin V-based radioligands, in particular ^{99m}Tc-Hynic-Annexin V, since this molecule is by far the most extensively investigated and best-characterised apoptosis marker at present. Furthermore, the newly emerging imaging modalities for in vivo detection of programmed cell death, such as MRI, MRS, optical, bioluminescent and ultrasound imaging, are briefly described. Finally, some future perspectives are presented with the aim of promoting the development of potential new strategies in pursuit of the ideal cell death-detecting radioligand.

Christophe M. M. Lahorte (✉)
Department of Radiopharmacy,
Faculty of Pharmaceutical Sciences,
Ghent University,
Harelbekestraat 72, 9000 Ghent, Belgium
e-mail: christophe.lahorte@ugent.be
Tel.: +32-9-2648065, Fax: +32-9-2648071

Keywords: Apoptosis – Programmed cell death – Annexin V – SPECT – PET

Eur J Nucl Med Mol Imaging (2004) 31:887–919
DOI 10.1007/s00259-004-1555-4

Introduction on cell death

Apoptosis is a common and universal mechanism of cell death, which was originally defined by Kerr et al. in 1972 [1] and has since been widely accepted by the scientific community. However, the first pathological descriptions of the cell death process date from the end of the nineteenth century. Although apoptosis and necrosis are commonly described as the two major cell death processes, there is also a third distinct but closely related form of cell death, referred to as oncosis; this term is employed to describe the pre-lethal stages of necrosis.

Necrosis or accidental cell death, including oncosis, is the most frequent type of cell death and is induced by a variety of sudden and severe non-physiological insults, including chemical or physical noxious insults and ischaemic or inflammatory injury. The process is characterised by progressive cell swelling, denaturation and coagulation of cytoplasmic proteins, disintegration of subcellular organelles and irreversible collapse of the plasma membrane integrity; this causes the release of cytotoxic cell components, thereby provoking an inflammatory response around the necrotic centre. In general, cell death by necrosis involves groups of cells and is often followed by the development of fibrotic tissue with distortion of the local tissue's architecture [2–4].

Apoptosis, however, is an energy-dependent, genetically controlled process by which cell death is activated through an internally regulated suicide program. In contrast with necrotic cell death, apoptosis tends to occur during less intense, chronic tissue insult. Once initiated,

apoptosis is characterised by a cascade of morphological and biochemical events which finally leads to the cell's demise if it has not previously been rescued by anti-apoptotic agents. The most prominent hallmarks of cells entering apoptosis include: phosphatidylserine (PS) externalisation, cytoplasm shrinkage, chromatin and nucleus condensation, DNA degradation and fragmentation of the cell into smaller "apoptotic bodies" by a budding process [5–8]. Finally, these membrane-enclosed bodies are engulfed and phagocytosed by macrophages and neighbouring cells, which then remove the cell fragments without inducing any concomitant inflammatory response. An unusual failure in this final clearance step may cause these cell fragments to degrade in a way similar to necrosis, leading to an inflammatory response, and is therefore defined as secondary necrosis. Thus, the apoptotic process can be divided into at least four functionally distinct phases: initiation, execution, degradation and elimination [9, 10].

Currently, two distinct types of pathway have been described by which apoptotic cell death is initiated: through death receptors or via the mitochondria. Nonetheless, both of these exclusive pathways eventually culminate in a mutual proteolytic cascade consisting of cystein aspartic acid-specific proteases (i.e. caspases), which act as executioners of the induced cell death process.

The death receptor pathway, also defined as the extrinsic cell death pathway, mainly consists of soluble or membrane-bound death ligands such as tumour necrosis factor α (TNF-α), Fas ligand (FasL) or TNF-related apoptosis-inducing ligand (TRAIL) which bind to their corresponding receptors. Subsequently, trimerisation of the receptor and binding to the cytoplasmic Fas-associated death domain adaptor protein (FADD) result in the formation of a death-inducing signalling complex (DISC). Finally, the DISC complex triggers the recruitment and activation of procaspase-8 and procaspase-3 followed by cleavage and activation of important downstream effector caspases such as procaspase-6, procaspase-8 and procaspase-10. These activated caspases cause cytoplasmic proteolysis and activation of DNAses which induce systematic degradation of nuclear DNA into multiple fragments of typically 180–200 bp [11, 12]. To date, seven types of death receptor have been described, including the Fas (CD95 or APO-1), TNF and TRAIL death receptor families [13–15].

On the other hand, the mitochondrial or intrinsic pathway is initiated by a variety of biochemical factors like oxidative and genotoxic stress, ischaemia, DNA damage, increased Ca^{2+} levels and chemotherapeutic drugs which provoke the release of pro-apoptotic factors like apoptosis-inducing factor (AIF), Smac, procaspases and cytochrome *c* from the mitochondria into the cytoplasm. Afterwards, the rise in cytoplasmic cytochrome *c* activates procaspase-9 and procaspase-3 consecutively, thereby resulting in a convergence with the death receptor pathway [12, 16]. AIF is able to proteolytically activate caspase-3 and nuclear endonucleases by itself. In contrast, cytochrome *c* requires interaction with additional proteins, including Apaf-1 (which binds ATP) and caspase-9 (Apaf-3), which together can activate procaspase-3. This complex of interacting proteins is called the "apoptosome".

Although distinctly different from each other in their initial phase, significant cross-talk between the extrinsic and intrinsic pathways has been demonstrated [17, 18]. This interaction is primarily possible due to a protein called Bid. In particular, once the death receptor pathway has been initiated, activated caspase-8 is able to truncate Bid, which in turn translocates to the mitochondria in order to contribute to cytochrome *c* release. Furthermore, both pathways are capable of inducing cell membrane alterations like PS externalisation in the early phase of apoptosis, through common activation of caspase-3.

Apoptosis is a highly conserved form of programmed cell death (PCD) that plays an important role in multiple physiological processes like organ development, tissue homeostasis and regulation of the immune system since many organisms use this mechanism to selectively eliminate unwanted cells. However, when the physiological balance between survival and death signals tilts towards cell death, the apoptosis program is engaged and culminates in a variety of pathological conditions (Table 1) [19–23]. Excessive apoptosis is known to result in progressive loss in tissue functionality, as occurs in acute myocardial infarction (AMI), chronic heart failure, allograft rejection, stroke, neurodegenerative disorders (e.g. Alzheimer's, Parkinson's and Huntington's disease) and inflammation. In contrast, autoimmune diseases like systemic lupus erythematosus (SLE) and rheumatoid arthritis are characterised by insufficient apoptosis, which enables immunologically competent cells (i.e. autoreactive lymphocytes) to survive and to injure healthy organs inappropriately. In addition, pronounced loss in normal apoptosis leads to excessive cell proliferation and subsequent tumour development [18, 24–27]. Furthermore, the beneficial or detrimental effect of many drugs can be attributed to their action on the apoptotic process [28–33]. Accordingly, non-invasive in vivo monitoring of the rate and extent at which apoptosis occurs, may provide clinicians with relevant clinical information on disease activity and therapeutic efficacy [34–36].

PS-targeting radioligands

Annexin V

Annexin V is a member of the calcium and phospholipid binding superfamily of Annexin proteins, of which at least 13 members have been identified in a variety of organisms in the animal and plant kingdoms [37–40]. Since the protein was originally found to possess vascular

Table 1. Medical fields for application of apoptosis imaging

Medical field	Pathological condition or medical application	References
Oncology	Chemotherapy-, radiation- or hormone-induced apoptosis monitoring in solid and haematological tumours	[25, 82, 83, 84, 258]
	Tumour detection (i.e. spontaneous apoptosis)	[24, 25, 26, 259, 260]
	Therapy response prediction (i.e. resistance to therapy)	[84, 261, 262]
Cardiology	Acute cardiac allograft rejection	[63, 136]
	AMI	[63, 263]
	Anthracycline-induced cardiotoxicity	[264, 265, 266]
	ARVD and skeletal muscle apoptosis	[21, 63, 267]
	CHF	[268, 269]
	CAD and atherosclerosis	[270, 271, 272]
	Infectious endocarditis (myocarditis)	[21, 63, 65]
	Intracardiac tumour growth	[70]
	Myocardial dysfunction	[63, 273, 274]
	Myocardial ischaemia—reperfusion injury	[155, 275, 276]
Transplant rejection	Allograft rejection of liver, lungs or heart	[277, 278, 279, 280]
Infection and Inflammation	Bacterial and viral infections	[19, 20, 22]
	MODS	[23]
	Septic shock	[23, 281]
Neurology	Cerebral ischaemia—reperfusion injury (stroke)	[282, 283]
	Neurodegenerative diseases: (Parkinson's, Alzheimer's, Huntington's disease, multiple and amyotrophic lateral sclerosis)	[284, 285]
	Trauma (spinal cord or brain injury)	[5, 286]
Metabolic diseases	Diabetes (type I)	[20]
Autoimmune diseases	Annexinopathies	[287]
	Rheumatoid arthritis	[288, 289]
	SLE	[202, 290]
	Inflammatory bowel disease	[291]
Skeletal diseases	Osteoarthritis	[20, 288]
Renal disease	Acute renal failure	[292, 293]
	Chronic renal atrophy and renal fibrosis	[293]
	Glomerular injury	[293]
	Polycystic renal disease	[23, 293]

AMI, Acute myocardial infarction; ARVD, arrhythmogenic right ventricle dysplasia; CAD, coronary artery disease; CHF, congestive heart failure; MODS, multiple organ dysfunction syndrome; SLE, systemic lupus erythematosus

anticoagulant activity, various synonyms have been used in the literature, including: placental protein 4 (PP4), placental anticoagulant protein I (PAP I), vascular anticoagulant protein alpha (VACα), lipocortin-V, endonexin II and calcium-dependent phospholipid binding protein (CaBP33) [41–44]. Like the other Annexin members, Annexin V is widely expressed in eukaryotic organisms. The protein is mainly found intracellularly on the cytosolic side of plasma membranes, although very low concentrations (1–6 ng/ml) circulate in the blood compartment of healthy humans [45, 46]. Furthermore, the protein is ubiquitously expressed in a variety of cell types, including: cardiomyocytes, vascular endothelium, erythrocytes, thrombocytes, lymphocytes, glial cells, astrocytes, oligodendrocytes, Schwann cells, skeletal muscles, hepatocytes, bronchi, chondrocytes and osteoblasts [45–51].

The mature Annexin V molecule consists of 319 amino acids with a total molecular weight of 35.8 kDa. The protein is folded into a planar cyclic arrangement with a unique N-terminal region followed by four homologous repeats of approximately 70 amino acids, each of which is composed of five alpha-helical segments. Similar to the other Annexin family members, every tandem repeat contains a highly conserved sequence of 17 amino acids, termed the "endonexin fold", which harbours a characteristic Ca^{2+}- and phospholipid- binding site [50–54]. Furthermore, the 3D structure of Annexin V is characterised by a concave and a convex side. The concave surface of the protein harbours the amino terminal tail and carboxy terminal tail, whereas the convex side bears the calcium binding sites located within the endonexin loop sequences.

Over the past years many studies have focussed on elucidating the biological functions of Annexins. Originally, Annexin V was found to exhibit potent vascular anticoagulant activity due to its inhibitory effect on prothrombin activation [55] and its ability to effectively prevent thrombus formation under normal physiological conditions. In addition, the protein is capable of inhibiting phospholipase A_2 (PLA_2) activity, thereby exerting anti-inflammatory properties due to its ability to prevent arachidonic acid release by PLA_2 [56, 57]. The protein also acts as an inhibitor of protein kinase C (PKC).

Most of the known biological functions of Annexin V can be attributed to its high affinity for negatively charged phospholipids in the presence of physiological concentrations of calcium. In particular, Annexin V is known to bind selectively with nanomolar affinity ($K_d \approx 0.5–7$ nM) to membrane bound PS residues [42, 55, 58]. Thus, PS binding of Annexin V not only proceeds very rapidly, but is also strongly dependent on the presence of Ca^{2+} ions. The molecular mechanism of action by which Annexin V binds to PS residues will be explained further (cf. ^{99m}Tc-Annexin V Mutants, below).

Based on these observations, Annexin V was originally labelled with different fluorescent tags (e.g. FITC) and is now routinely used for histological and cell-sorting studies to identify and quantify apoptotic cells [59–62]. However, all of these detection methods (i.e. microscopy, immunohistochemistry, flow cytometry) are either characterised by specific problems in detectability or exhibit restricted applicability in vitro and often require invasive sampling techniques like biopsies [63–66]. Other methods like the TUNEL assay (terminal uridine deoxynucleotidyl end-labelling) often lack sensitivity in quantifying the process since their detection mechanism only targets cells in a later stage of the apoptosis cascade, when phagocytosis of apoptotic cells is already occurring in vivo.

In analogy, Annexin V can also be radiolabelled with radionuclide tags such as ^{99m}Tc or ^{123}I for non-invasive detection and quantification of apoptosis in vivo [67–70]. Initial in vitro studies with normal and sickle-cell erythrocytes, activated blood platelets and tissue factor (TF)-expressing fibroblasts or ovarian carcinoma cells clearly demonstrated the proof of concept that early apoptosis could be detected successfully with radiolabelled Annexin V [71]. Since then, extensive progress has been made in the in vivo evaluation of radiolabelled Annexin V in animals and humans and in the development of alternative cell death radioligands.

Annexin V was originally isolated from placental tissue of human or other origin [72, 73]. However, recombinant human Annexin V (rh-Annexin V) is currently being produced by cytoplasmic expression in *Escherichia coli* [74–76]. Due to its fairly low molecular weight, the recombinant protein can easily be generated in high (i.e. milligram) yields with excellent purity and is very unlikely to trigger an immune response compared with murine monoclonal antibodies or murine/bovine Annexin V. Furthermore, unlike Annexin V originating from human placentas, rh-Annexin V can be considered practically free of human plasma constituents while containing extremely low endotoxin levels, allowing its use in various clinical applications.

PS expression as a cell death target

According to the existing major cell death pathways described in the literature, several of the involved processes may serve as a specific target for new apoptosis radioligands, including: PS exposure, caspase activation, mitochondrial permeability transition, FasR expression, and TNF-α-mediated cell death. Until now, interest has focussed on the phenomenon of PS externalisation. In general, eukaryotic plasma membranes exhibit significant phospholipid asymmetry, with choline-containing phospholipids such as phosphatidylcholine (PC) and sphingomyelin (SM) mainly being expressed on the extracellular side of the cell. In contrast, aminophospholipids like PS and phosphatidyl ethanolamine (PE) are largely confined to the inner side of the phospholipid bilayer, representing the two major lipid components in this compartment. In fact, PS residues are the only phospholipids which are virtually absent on the outer cell membrane layer [77, 78]. This asymmetrical phospholipid distribution is regulated enzymatically by aminophospholipid translocase activity which catalyses the transportation of PS and PE residues from the outer to the inner leaflet of the cell membrane under normal cellular conditions. Conversely, a second enzyme called scramblase controls the bidirectional transbilayer movement of all phospholipids [79–81].

One of the early hallmarks of cells entering the apoptosis cascade is the fast externalisation of PS residues from the cytoplasmic to the extracellular side of the membrane. This PS surface exposure results from a deactivation in the translocase and floppase activity in combination with an enhanced scramblase activity (Fig. 1). Although many chemical (e.g. chemotherapeutics, glucocorticoids) [82–84], physical (e.g. UV radiation, γ-radiation, heat) [85–87] and biochemical factors (e.g. hypoxia, osmotic imbalance, high Ca^{2+} levels, nitrogen oxide) [88] are able to induce apoptosis in vitro and in vivo, the basic mechanism of PS expression on the membrane of cells entering apoptosis always proceeds regardless of the apoptosis-inducing agent or cell type [89, 90]. Most interestingly, PS externalisation precedes most of the other events within the apoptosis cascade, including: cytoplasm shrinkage, condensation of the nucleus, DNA degradation and fragmentation of the cell into smaller apoptotic bodies [89–91]. Since the membrane-engulfed cell fragments are removed by phagocytic cells in the final stage of apoptosis, externalisation of PS residues to the surface of dying cells acts as a

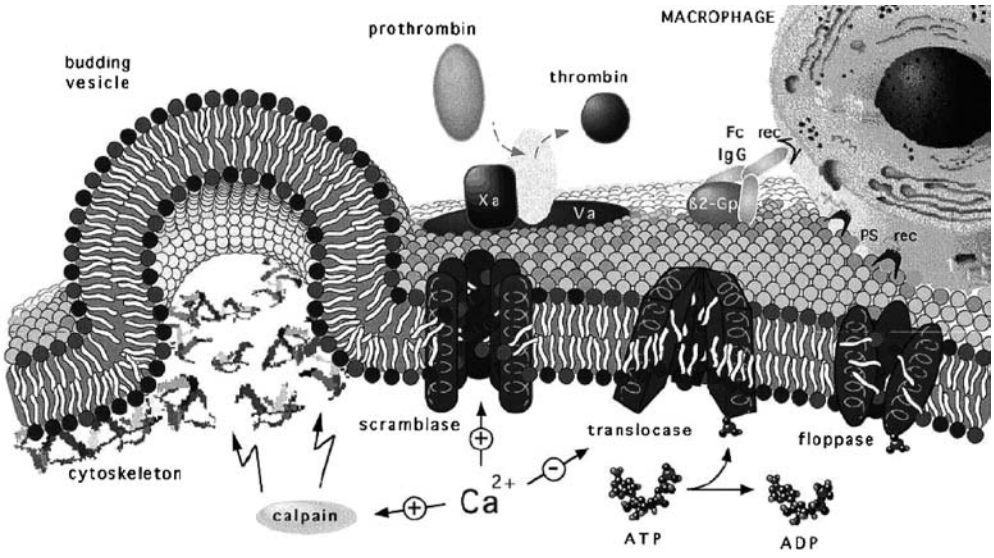

Fig. 1. The regulation and physiology of membrane PS asymmetry. This model depicts how the membrane PS asymmetry is generated and drastically altered in PS-related (patho)physiological processes such as blood coagulation (including thrombocyte activation), thrombosis and apoptotic cell death. At physiological Ca^{2+} concentrations, the asymmetrical phospholipid distribution is enzymatically promoted by translocase and floppase activity and inactive scramblase. The ATP-dependent aminophospholipid-specific translocase catalyses the transportation of PS residues and PE residues from the outer to the inner leaflet of the cell membrane. Conversely, the ATP-dependent non-specific lipid floppase slowly transports lipids from the cell's inner to outer side whereas the Ca^{2+}-dependent non-specific lipid scramblase controls the bidirectional transbilayer movement of all phospholipids. Elevated intracellular Ca^{2+} levels will facilitate membrane blebbing through calpain activation and induce PS externalisation by providing a deactivation in the translocase and floppase activity in combination with an enhanced scramblase activity. Subsequently, the apoptotic cells which express PS residues are recognised and eliminated by macrophages (adapted from Zwaal and Schroit [80])

"recognition and elimination" signal for macrophages which express the PS receptor [92–94]. Concordantly, apoptotic cell death represents a dynamic process, which provides a temporary time window for detection in vivo.

The number of PS-binding sites for Annexin V on human erythrocytes and resting platelets has been reported as 278 and 5,000 sites/cell, respectively, [95–97]. However, this number significantly increases to 2×10^5/cell for activated blood platelets and 8.8×10^6 per cell in the case of endothelial cells [98], whereas apoptotic tumour cells have been shown to express up to $6–24\times10^6$ sites/cell [99]. Taking into account the stoichiometry of Annexin V binding to PS residues, four to eight Annexin V molecules are able to bind per exposed PS residue [100]. Hence, considering all these findings, the loss of PS asymmetry constitutes a very attractive target for early in vivo detection of PCD. Consequently, about 90% of the currently developed apoptosis radioligands consist of Annexin V-based PS-targeting molecules. Additionally, fast translocation of PS residues to the outer side of the cell membrane is also known to take place in sickle-cell erythrocytes and during the process of blood platelet activation since PS expression is essential for the platelet pro-coagulant activity. Therefore, fluorescent or radiolabelled Annexin V also appears very promising for in vivo detection of atherosclerotic plaques or thrombi which contain high amounts of activated platelets and apoptotic monocytes [96, 101–103].

With regard to the specificity of apoptosis detection by PS targeting, one should take into account the fact that cells dying by necrosis will also allow binding with Annexin V ligands since the intracellular PS residues become readily accessible for binding as soon as the plasma membrane ruptures. Consequently, in vivo discrimination between apoptotic and necrotic cell death using PS-targeting radioligands will be very difficult.

Radiolabelled Annexin V derivatives

Halogenated Annexin V

Annexin V and its derivatives have been labelled with most halogens, including ^{123}I, ^{125}I, ^{124}I and ^{18}F, thereby providing a broad range of imaging applications in apoptosis research from single-photon emission computed tomography (SPECT) and autoradiography to positron emission tomography (PET). Somewhat similar to the group of ^{99m}Tc-Annexin V radioligands, halogenated Annexin V was produced by either direct or indirect radiolabelling methods, as described below.

^{123}I/^{125}I-Annexin V. Direct iodination of proteins and peptides by means of electrophilic aromatic substitution of the molecule's tyrosine residues has been used in radiochemistry for many years owing to the simplicity and

easiness of the technique. The most commonly used techniques are the IodoGen, IodoBead, chloramine-T (CAT) or enzymatic lacto-, bromo- or myeloperoxidase methods.

Preparation of ^{123}I-Annexin V and ^{125}I-Annexin V using the IodoGen method [104] was originally described by the group of Tait et al. in the early 1990s [96]. Iodination of Annexin V usually consisted of a one-pot reaction in which the protein was radiolabelled at pH 7.5–8 at room temperature, using IodoGen-coated reaction vials, after which the reaction was quenched with sodium metabisulphite and/or NaI. Additional purification of the radioligand by gel filtration or extensive dialysis resulted in excellent radiochemical purities of greater than 99% while retaining full anticoagulant and phospholipid binding activity [105–107]. Only one study has reported so far on the preparation of ^{125}I-Annexin V by means of the enzymatic lactoperoxidase-glucose oxidase method [108]. Similar to the IodoBead method, enzyme-coated beads were applied in this approach as solid phase oxidant generating significantly higher specific activities. Although radiolabelling of Annexin V according to the IodoGen or enzymatic method was not optimised, ^{123}I/^{125}I-Annexin V was used in many in vitro and in vivo studies for several years and its usefulness in detecting PS expression was clearly demonstrated. Most in vitro studies with iodinated Annexin V consisted of radioligand binding assays with normal and sickle-cell erythrocytes [74, 105], activated blood platelets [95, 96, 107, 108] and tissue factor (TF)-expressing fibroblasts [109] or ovarian carcinoma cells [110]. Originally, radioiodinated Annexin V was tested ex vivo as a potential platelet-directed thrombus imaging agent in rabbits and swine [76, 101, 106]. ^{125}I/^{123}I-Annexin V selectively targeted thrombi in rabbit iliac and swine carotid arteries, resulting in thrombus/blood ratios of 6.4 and 6.9, respectively, within 2 h post injection (p.i.). Left atrial thrombi were found to provide even higher thrombus/blood uptake ratios, of ca. 13.4, indicating the presence of a stronger detection signal in acutely formed intracardiac thrombi compared with thrombi induced in arteries. Other groups even developed prourokinase-Annexin V chimeras as potential thrombolytic agents based on the ability of Annexin V to bind activated platelets in thrombi with high affinity [111].

Thorough optimisation of the radiolabelling procedure for ^{123}I-Annexin V was described by Lahorte et al. for both the IodoGen and the IodoBead method [112, 113]. Using recombinant human Annexin V, optimisation of all reaction parameters resulted in radiochemical yields of 75–85%, respectively, while preserving sufficient biological activity towards blood platelets and apoptotic lymphocytes. In addition, excellent radiochemical purities of >98% were obtained for both methods. Most interestingly, further improvement of the IodoGen method allowed routine production of clinical-grade ^{123}I-Annexin V, achieving radiochemical yields of 87% and specific activities of 13.4 GBq/μmol [114]. Preliminary studies in a rat model of sepsis-induced myocardial dysfunction clearly indicated significantly increased radioligand uptake in the myocardium compared with control animals [115]. Furthermore, myocardial tracer uptake could be decreased by about 80% by means of broad-spectrum and selective caspase-3 inhibitors, thereby providing evidence for the specificity of the tracer signal [116, 117]. Most recently, the biodistribution and dosimetry of ^{123}I-rh-Annexin V was evaluated in humans and compared with previously obtained data in mice applying the MIRD program [114]. ^{123}I-rh-Annexin V was characterised by a fast bi-exponential clearance from the blood compartment (i.e. $T_{1/2,\alpha} = 3.87 \pm 0.90$ min and $T_{1/2,\beta} = 4.13 \pm 2.04$ h) and predominant uptake in the kidneys, liver and gastrointestinal tract followed by pronounced renal excretion. However, delayed whole-body images indicated progressive deiodination of the radioligand, which could impede in vivo detection of apoptosis in the abdominal region. From the dosimetry point of view, intravenous injection of 345 MBq ^{123}I-rh-Annexin V resulted in moderate radiation doses for most organs, whereas the estimated effective dose received by the volunteers in this study represented 0.02 mSv/MBq administered. Thus, the effective dose received by the volunteers in this study (i.e. on average 6.9 mSv) is somewhat higher than the 5 mSv upper limit average effective dose of category IIa of the World Health Organisation and category IIb of the ICRP report [118, 119]. The results of this study also demonstrated that ^{123}I-rh-Annexin V was well tolerated in humans (n=6) without provoking any adverse effects or complications despite the relatively high amount of radiolabelled protein delivered as bolus injection (i.e. 940±64 μg/volunteer). In addition, for most organs, the estimated absorbed radiation dose as well as the estimated effective dose for humans corresponded well with the extrapolated radiation dose estimates originating from the animal biodistribution studies.

Alternatively, Annexin V has been iodinated indirectly by applying the commonly known Bolton-Hunter method and compared with directly iodinated Annexin V prepared by the IodoBead method [120]. Iodination of the water-soluble Bolton-Hunter reagent with CAT and subsequent conjugation to Annexin V for 1 h at pH 9.2 resulted in relatively poor radiochemical yields of 40%. In vitro assays with irradiated neuroblastoma cells and immobilised PS residues indicated 50–75% preservation of the radioligand's PS-binding capacity. However, Bolton-Hunter-labelled ^{125}I-Annexin V showed clearly improved in vivo stability compared with directly ^{125}I-labelled Annexin V at 2 h p.i. Furthermore, C3H mice treated with anti-Fas monoclonal antibody (MoAb) or irradiation showed significantly increased activity accumulation in the apoptotic organs. However, the Bolton-Hunter radioligand showed extensive accumulation in the liver and bowels owing to increased lipophilicity, which could seriously hamper in vivo apoptosis detec-

tion in these regions. So, although the Bolton-Hunter approach seems to offer improved in vivo stability over directly iodinated Annexin V, the method remains laborious and time-consuming while providing low radiochemical yields. Furthermore, the inherent biological behaviour of Bolton-Hunter-labelled Annexin V could restrict its applicability for apoptosis imaging in the abdominal region.

[^{124}I]Iodoannexin V, [^{124}I]m-IBA-Annexin V, ^{124}I-MBP-Annexin V and ^{124}IB-MBP-Annexin V. Additionally to the gamma-emitting radionuclides ^{123}I and ^{125}I, Annexin V has also been radiolabelled with the positron emitter ^{124}I (physical half-life of ^{124}I=4.18 days, $E_{max}\beta^{+}$=1.53, 2.14 MeV), by either direct or indirect iodination. In a first study, Glaser et al. reported on the ^{124}I labelling of wild-type and polyhistidine-tagged recombinant Annexin V using two different methods [121, 122]. The modified Annexin V protein contained a tag with a tobacco etch virus (TEV) protease cleavage site linked to a hexahistidine residue. Both proteins were iodinated directly by using a variant of the well-established chloramine-T (CAT) method and optimised for reaction time and pH. When using a 10-min reaction time at pH 6.5, instant thin-layer chromatography (ITLC) analysis of the reaction mixtures indicated that nearly 80% of the radioactivity was incorporated with both unmodified and polyhistidine-tagged Annexin V, resulting in a 97.7%± 1.0% radiochemical purity (RCP) and a specific activity of 14.5 GBq/μmol post purification. In spite of this relatively high radiochemical yield and specific activity, a poor overall yield of ca. 22.3%±2.6% was obtained for ^{124}I-Annexin V after purification by means of gel filtration on a Sephadex column. Regardless of the higher RCP (>99%) obtained by fast protein liquid chromatography (FPLC) purification, the loss of radioligand was even more pronounced in such cases, indicating significant adsorption of the iodinated protein to the packing material of the TSK G3000 SWxl size exclusion column. In addition, direct iodination of Annexin V by means of CAT instead of IodoGen initially resulted in even lower radiochemical yields of near 4–6% [121].

Since Annexin V contains 21 lysine residues, the indirect iodination approach with N-acylation of amino residues was also investigated. For this purpose, Glaser et al. applied the pre-labelled reagent *N*-succinimidyl 3-[^{124}I]iodobenzoate ([^{124}I]m-SIB), generated from the stannyl precursor *N*-succinimidyl 3-(trimethylstannyl)-benzoate (m-MeATE) in order to produce [^{124}I]m-IBA-Annexin V with a high RCP of 96.7%±2.1% by means of a three-step procedure. The [^{124}I]iododestannylation step was performed using IodoGen as solid phase oxidant whereas the final reaction step consisted of [^{124}I]m-SIB conjugation to the protein at pH 8.5. Similar to the direct labelling approach, [^{124}I]m-IBA-Annexin V was obtained in poor overall radiochemical yields after purification by FPLC and gel filtration (i.e. 14% and 25%, respectively), which was, in part, attributed by Glaser et al. to the formation of unidentified radioactive side-products which are retained on the purification column. Efforts to increase the recovery of radiolabelled protein by using PBS primed with BSA during gel filtration provided only very limited success (i.e. 34% radiochemical yield). However, subsequent to the modified purification conditions the RCP dropped back to merely 76%, mainly due to poor column performance.

Furthermore, the specific activity of [^{124}I]m-IBA-Annexin (i.e. 1.6 GBq/μmol) was ninefold lower than that of directly ^{124}I-labelled Annexin V and seems inherently linked to the use of multiple reaction steps involved in the indirect labelling approach. In particular, the pre-labelled active ester [^{124}I]m-SIB is produced in a low and variable radiochemical yield (i.e. 39.3%±8.4% after HPLC purification) and can be considered as a major contributor to the low specific activity of the final [^{124}I]m-IBA-Annexin V product. Nevertheless, [^{124}I]iodoannexin V and [^{124}I]m-IBA-Annexin V showed comparable in vitro stability (i.e. both compounds were stable up to 4 days when stored in PBS at 4°C, after which deiodination started to proceed). However, [^{124}I]m-IBA-Annexin V should be expected to show superior stability over directly labelled Annexin V when uploaded with higher activities. The biological activity of both molecules was subjected to preliminary testing in an in vitro model of camptothecin-induced apoptosis in HL60 cells by using the ^{125}I counterparts of directly and indirectly iodinated Annexin V. Human leukaemic HL60 cells pre-treated for 6 h with campothecin showed increases in tracer uptake of 17% and 21% for [^{125}I]iodoannexin V and [^{125}I]m-IBA-Annexin V, respectively, compared with control cells. However, statistical significance for the 17% increased [^{125}I]iodoannexin V binding was found in only one out of three experiments. Nevertheless, binding of [^{125}I]m-IBA-Annexin V to control and pre-treated cells could be blocked by 60% and 68%, respectively, by pre-incubation with a 100-fold excess of unlabelled Annexin V. Based on these first in vitro results, one can conclude that these two radioligands seem to exhibit a rather comparable biopotency. However, when interpreting these data, it needs to be underscored that the minor difference in apoptosis observed between control and campothecin-treated cells (as reflected by the tracer binding) either indicates an inferior biopotency of the tracer or demonstrates that the DMSO solvent used for dissolving campothecin is capable of inducing apoptosis in the control cells to almost the same extent as in the campothecin-treated cells. Since [^{125}I]m-IBA-Annexin V binding to control and pre-treated cells could be blocked to a similar extent (i.e. by 60% and 68%, respectively) by pre-incubation with a 100-fold excess of unlabelled Annexin V, the second hypothesis seems to be most likely. In this case the choice of in vitro model was less appropriate or the model would require further improvements and validation by alternative tech-

niques to assess the amount of induced apoptosis accurately. This assumption was confirmed by a second in vitro model in which heat-induced PS exposure on HL60 cells resulted in a significant increase (i.e. by 56%) in [^{124}I]m-IBA-Annexin V binding compared with control cells, thereby proving the biopotency of the radioligand [121].

From a clinical point of view, the long physical half-life of ^{124}I offers broad possibilities for the (in)direct iodination of Annexin V and would allow monitoring and quantification of long-term biological processes. In contrast, in vivo administration of long-living ^{124}I-labelled Annexin V to humans could contribute to high radiation doses to specific organs such liver, which is generally known to metabolise radiolabelled proteins, and subsequent accumulation of free iodine-124 in the thyroid and stomach due to deiodination of the protein. In this regard, ^{124}I-labelled Annexin V ligands should display good in vivo stability and sufficient clearance from the body over time in order to minimise radiation burden to the patient, especially when considering the complex decay scheme of ^{124}I, which produces several high-energy gamma emissions (0.60–1.69 MeV). Another disadvantage of the isotope that needs to be addressed is the low ratio of disintegrations, which results in 23% positrons, thereby requiring higher tracer doses to the patient or longer acquisition times in order to obtain high-quality PET scans.

Most recently, a third type of ^{124}I-Annexin V ligand was developed by Keen and Dekker et al., consisting of a maltose binding protein-Annexin V chimera (MBP-Anx 5) [123]. The molecule was radiolabelled by direct iodination applying the IodoGen method and evaluated in a mouse model of anti-Fas MoAb-induced hepatic apoptosis together with unmodified Annexin V, while iodinated MBP and albumin were used as corresponding control proteins. BDF1 mice pre-treated with anti-Fas MoAb 4 h prior to the tracer injection showed significantly increased hepatic apoptosis compared with control animals as determined morphologically. Furthermore, a correlation was found between the apoptotic index and the elevated liver uptake of both ^{124}I-Annexin V and ^{124}I-MBP-Anx 5 but not with that of the control proteins. Moreover, camptothecin-treated Jurkat cells had previously been demonstrated to exhibit an eightfold increase in ^{124}I-MBP-Anx 5 binding compared with non-treated cells [124]. In spite of these promising results, the biodistribution of directly labelled ^{124}I-MBP-Anx 5 in both normal and anti-Fas-MoAb-treated mice was characterised by rapid and extensive dehalogenation, as reflected by activity accumulation in the thyroid [123, 124]. This major drawback prompted Dekker et al. to iodinate MBP-Anx 5 indirectly by using [^{124}I]-4-iodobenzylsuccinimide as a precursor molecule, which resulted in ^{124}IB-MBP-Anx 5, applying the IodoGen method [125]. Comparative biodistribution experiments in normal mice at 2 h post tracer injection demonstrated significantly increased liver- and kidney-to-blood uptake ratios of ^{124}IB-MBP-Anx 5 versus ^{124}I-MBP-Anx 5. In contrast, urinary excretion was substantially lower in the case of ^{124}IB-MBP-Anx 5, reflecting inferior renal excretion which could contribute to elevated residual background activity in the body. These preliminary data indicate that poor image contrast can be expected in the gastrointestinal region within the first few hours of tracer administration, which would seriously hamper clinical use. Furthermore, it remains unclear whether indirectly iodinated MBP-Anx 5 possesses better stability to in vivo dehalogenation compared with ^{124}I-MBP-Anx 5 since the thyroid of all investigated animal groups was blocked prior to tracer injection [125].

In conclusion, preliminary in vitro and vivo results have provided the first evidence on the potential applicability of ^{124}I-labelled Annexin V as a PET probe for imaging of apoptosis. Nevertheless, many of the problems mentioned above will need to be overcome before ^{124}I-labelled Annexin V, prepared by either direct or indirect iodination, could find its way into the clinic.

4-[^{18}F]fluorobenzoylannexin V. Similar to the indirect radiolabelling method for [^{124}I]m-IBA-Annexin V, a four-step synthesis has been described by three different research groups for production of 4-[^{18}F]fluorobenzoyl-annexin V (4-[^{18}F]FBA) by means of the *N*-succinimidyl-4-[^{18}F]fluorobenzoate ([^{18}F]SFB) precursor. The majority of the radiolabelling approaches have been based on the method of Wester et al. making use of ethyl-4-[^{18}F]fluorobenzoate, 4-[^{18}F]fluorobenzoic acid and [^{18}F]SFB as intermediates [126, 127]. Although the same intermediate reaction products were generated in all methods mentioned below, different reagents, reaction conditions and purification methods were used in some of the synthesis steps, resulting in different overall radiochemical yields. The most technically advanced method was described by Zijlstra et al. making use of a microcomputer-controlled, automated module producing 4-[^{18}F]FBA within 90 min in radiochemical yields of 15–20% (i.e. decay corrected) and with an RCP of at least 95%. Additionally, specific activities of more than 35 GBq/μmol were achieved, which is significantly higher than the value reported for ^{124}I-labelled Annexin V [128]. Despite the low overall yield, 4-[^{18}F]FBA could be prepared by the automated system in batches of up to 2 GBq when starting from 25 GBq [^{18}F]fluoride [129]. In contrast, the group of Mease et al. obtained significantly higher radiochemical yields ranging from 38% to 68%, in correspondence with an increased Annexin V concentration (i.e. 1.25–5 μg/μl) used for conjugation to [^{18}F]SFB [130]. One of the major contributors to this difference is the 52–55% yield in which [^{18}F]SFB could be produced compared with the 35% yield obtained by Zijlstra et al. Further optimisation of the [^{18}F]SFB precursor synthesis resulted in radiochemical yields of up to 77% [131]. On the other hand, the third method present-

ed by Murakami et al. for production of 4-[^{18}F]FBA requires 2 h of synthesis while generating the lowest radiochemical yields, in the range of 10%, with 99% RCP [132].

In vitro biological activity of 4-[^{18}F]FBA was initially verified by Zijlstra et al. towards PS-containing liposomes and UV-irradiated Jurkat T-cell lymphoblasts. 4-[^{18}F]FBA showed rapid and highly specific binding to liposomes containing 80–85% of PS residues whereas the Jurkat T-cell study revealed at least 60% increased tracer binding over time to apoptotic T cells versus non-apoptotic T cells. Furthermore, radioligand binding appeared to be time- and concentration-dependent and could be saturated. Mease and Grierson et al. demonstrated retention of the tracer's biological activity in a red blood cell assay in which 4-[^{18}F]FBA binding to externalised PS residues was confirmed. In fact, 4-[^{18}F]FBA exhibited a nanomolar affinity for red blood cells (K_d≈10.8±5.0 n*M*) [131]. At present, Murakami et al. were the first to evaluate ^{18}F-labelled Annexin V in vivo in a rat model of myocardial ischaemia-reperfusion. Twenty-four hours after inducing ischaemia, a fourfold increase in tracer uptake in the infarcted area was seen compared with normal myocardial tissue. Specificity of the apoptotic signal was confirmed by the co-localisation of TUNEL-positive cells in the area of tracer accumulation. Most recently, preliminary biodistribution studies in normal Sprague-Dawley rats indicated that 4-[^{18}F]FBA is rapidly cleared from liver, kidneys and heart within 1 h p.i., and provides high urinary excretion [131]. Moreover, 4-[^{18}F]FBA PET images at 45 min p.i. did not show any thyroid uptake, which might reflect ongoing dehalogenation.

Based on the available data, 4-[^{18}F]FBA seems to offer promise as a potential tool for PET imaging of PCD. PET studies with positron-emitting Annexin V radioligands not only could enhance the sensitivity and spatial resolution but would also allow better localisation and quantification of apoptotic areas compared with SPECT studies. Furthermore, ^{18}F (physical half-life of ^{18}F=1.83 h, $E_{max}\beta^+$=0.635 MeV) possesses a much shorter half-life and lower energetic positron emission compared with ^{124}I, which is likely to contribute to a lower radiation burden to the patient considering the apparent superior biological clearance of 4-[^{18}F]FBA.

^{99m}Tc-Annexin V

Beyond any doubt, ^{99m}Tc-Annexin V as a marker of PS expression is by far the most extensively investigated and broadly used apoptosis-detecting radioligand to date. Over recent years, numerous ^{99m}Tc-Annexin V radioligands have been developed by different groups using different types of chelators and co-ligands, each resulting in a different biological behaviour. The popularity and high interest in this group of Annexin-based radioligands

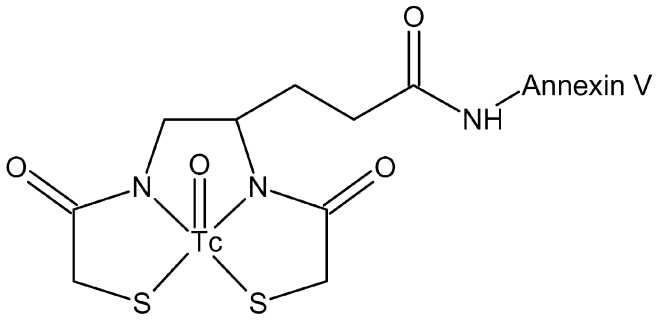

Fig. 2. Chemical structure of ^{99m}Tc-N_2S_2-Annexin V (^{99m}Tc-BTAP-Anx V)

is in part due to the substantial advantages of ^{99m}Tc compared with many other radionuclides. The ^{99m}Tc isotope is characterised by optimal radionuclidic properties for SPECT imaging (physical half-life of ^{99m}Tc=6.01 h, $E_{max}\gamma$=0.141 MeV), is inexpensive and is easily available. A thorough overview and discussion of the currently existing direct and indirect ^{99m}Tc-labelling methods for Annexin V and its derivatives is presented hereafter.

^{99m}Tc-BTAP-Annexin V. About 4 years after the development of radioiodinated Annexin V, ^{99m}Tc-4,5-bis-(thioacetamido)pentanoyl-Annexin V (^{99m}Tc-BTAP-Anx V) became the first ^{99m}Tc-Annexin V radioligand to be described (Fig. 2). ^{99m}Tc labelling of Annexin V was performed according to the pre-formed chelate approach in which a diamide dimercaptide N_2S_2 chelate was used, based on the OncoTrac labelling method originally described by Kasina et al. [133, 134]. For this purpose, ^{99m}Tc was first converted in the presence of stannous gluconate to ^{99m}Tc-gluconate and reacted with the acidified phenthioate ligand under heating to form a stable ^{99m}Tc-N_2S_2 complex. In a final step, the ^{99m}Tc-N_2S_2-TFP ester was conjugated to the protein at basic pH, after which the radioligand was purified by gel filtration, resulting in 25–30% overall radiochemical yields and a specific activity of 58.3 GBq/μmol. Subsequently, the production of ^{99m}Tc-N_2S_2-Annexin V was further optimised in a kit formulation (Apomate, Theseus Imaging Corporation, Boston, USA) and evaluated in vivo in Yorkshire swine [101] and patients with acute cardiac transplant rejection [135, 136].

Initial studies in a swine model of trial thrombi indicated the potential use of ^{99m}Tc-BTAP-Anx V as a selective thrombus targeting agent generating thrombus/blood uptake ratios of 14.2, comparable to ^{125}I-Annexin V [101]. More importantly, however, ^{99m}Tc-BTAP-Anx V provided the first evidence that in vivo detection of PS expression by means of SPECT was feasible. Early planar and tomographic images acquired within 140 min p.i. showed increasing tracer uptake over time in intracardiac thrombi, resulting in three- to fourfold higher uptake compared with control animals. Phase I clinical studies

investigating the biodistribution and dosimetry of ^{99m}Tc-BTAP-Anx V in a variety of patients clearly indicated predominant accumulation of radioactivity in the kidneys, liver and urine bladder over time [137]. However, the radioligand showed fast and extensive bowel excretion, precluding its clinical use for imaging apoptosis in the abdominal region. The high accumulation of radioactivity in the gastrointestinal tract as reported for ^{123}I-rh-Annexin V was even more pronounced for ^{99m}Tc-BTAP-Anx V. Nevertheless, ^{99m}Tc-N_2S_2-Annexin V has proven most useful for in vivo detection of apoptotic and necrotic cell death in patients with acute cardiac transplant rejection [135, 136] and intracardiac tumours [70]. Furthermore, the radioligand has been used successfully to assess chemotherapy- and radiotherapy-induced apoptosis in patients with lung and breast cancer [35, 138] or lymphomas [139].

From the radiopharmaceutical point of view, the ^{99m}Tc-BTAP-Anx V kit formulation containing 11 kit components remains very elaborate and time-consuming since it requires multiple reaction steps at different temperature and pH conditions and a rather complex purification procedure. Furthermore, the preparation requires high (i.e. 4.4–5.5 GBq) start activities of ^{99m}Tc, thereby increasing the radiation exposure to the operator, while providing low radiochemical yields. For this multitude of reasons, an improved ^{99m}Tc-Annexin V ligand was required to address the major drawbacks of ^{99m}Tc-BTAP-Anx V.

^{99m}Tc-Hynic-Annexin V. In search of an alternative radiolabelling approach for Annexin V, the group of Blankenberg et al. applied the Hynic technology in 1998, which was originally developed by Abrams et al. [140]. The hydrazino-nicotinamide (Hynic) ligand, as a nicotinic acid analogue, is a bifunctional chelator capable of binding to the NH_2-terminal amino acid and lysine residues of proteins on the one hand and of sequestering ^{99m}Tc on the other. Using tricine as co-ligand, the Hynic-Annexin V conjugate proved a most stable complex and allowed fast and efficient labelling with ^{99m}Tc in the presence of stannous ions (Fig. 3A). Consequently, the one-step reaction provides ^{99m}Tc-Hynic-Annexin in high radiochemical yields of typically 92–95% without requiring any additional purification step. Most interestingly, using the Hynic methodology, the Annexin V protein can be "uploaded" with ^{99m}Tc to very high specific activities of 198–265 GBq/μmol, making it most useful for in vivo imaging applications [141]. The radiolabelling procedure was further improved into a kit formulation of two vials requiring only 15 min of reaction (^{99m}Tc-Hynic-Annexin V, Theseus Imaging Corporation, Boston, USA). In comparison with ^{99m}Tc-N_2S_2-Annexin V, the ^{99m}Tc-Hynic-Annexin V formulation offers a much simpler and faster preparation at room temperature, while providing significantly higher radiochemical yields. Consequently, the radiolabelling method requires substantially lower start activities (e.g. 1.11–1.48 GBq), thereby improving radiosafety to the operator. All these advantages make ^{99m}Tc-Hynic-Annexin V much more suitable for routine production and fast application in a clinical setting. The coming of age of this second-generation kit represented a prelude to the impressive armamentarium of Annexin V-based radioligands that has been continuously expanding since then.

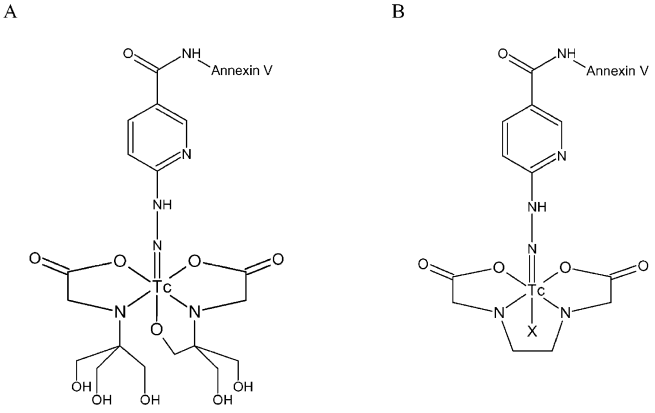

Fig. 3A, B. Chemical structures of ^{99m}Tc-Hynic-derivatised Annexin V using either tricine or EDDA as co-ligand: **A** ^{99m}Tc-Hynic(tricine)$_2$-Annexin V, **B** ^{99m}Tc-Hynic-EDDA-Annexin V (^{99m}Tc-EDDA-Hynexin)

Undoubtedly, the development of ^{99m}Tc-Hynic-Annexin V can be considered as a benchmark in the field of apoptosis imaging since this tracer is by far the most extensively investigated and best characterised apoptosis-detecting radioligand thus far (Table 2). Numerous in vivo studies in animals have been published, demonstrating the broad applicability of ^{99m}Tc-Hynic-Annexin V as a SPECT radioligand for imaging apoptotic cell death. Initially the radioligand was successfully used in animal models of Anti-Fas MoAb-induced hepatic apoptosis, allograft rejection of the heart liver and lungs, myocardial ischaemia-reperfusion injury, anthracycline-induced cardiomyopathy, rheumatoid arthritis, sterile inflammation, hypoxic brain injury and cyclophosphamide-induced intramedullary apoptosis [67, 142].[1] Moreover, Narula et al. provided first evidence that internalisation of ^{99m}Tc-labelled Annexin V in ischaemic myocardial tissue exceeds 50%, probably due to translocation of PS residues back to the inner sarcolemmal leaflet upon reperfusion [143]. Most interestingly, ^{99m}Tc-Hynic-Annexin V is increasingly being applied to monitor and evaluate the therapeutic effect of cardioprotective and immunosuppressive agents based on their ability to protect specific cells against apoptotic cell death [144, 145]. Conversely, the apoptosis marker has shown great potential for in vivo monitoring and prediction of anti-cancer treatment response.

[1] A detailed list of preclinical studies is available from the author.

Table 2. List of clinical trials (phase I/III)

(Radio) ligand	Type of study	References
^{123}I-Annexin V	Biodistribution and dosimetry in volunteers	[114]
^{99m}Tc-Hynic-Annexin V	AMI patients	[147, 148, 149]
^{99m}Tc-Hynic-Annexin V	Biodistribution and dosimetry study in volunteers	[146]
^{99m}Tc-Hynic-Annexin V	Follicular lymphoma patients receiving radiotherapy	[139]
^{99m}Tc-Hynic-Annexin V	Head and neck carcinoma patients	[151, 152]
^{99m}Tc-Hynic-Annexin V	Intracardiac tumours and infectious endocarditis	[150]
^{99m}Tc-Hynic-Annexin V	NSCLC patients receiving platinum-based chemotherapy	[138]
^{99m}Tc-Hynic-Annexin V	Reversible ischaemic injury and IP-induced apoptosis in the non-dominant forearm of volunteers	[294]
^{99m}Tc-i-Anx V	AMI patients	[69]
^{99m}Tc-i-Anx V	Biodistribution and dosimetry study in volunteers and patients with MI and Crohn's disease	[153]
^{99m}Tc-MIBI	^{99m}Tc-MIBI efflux study in apoptotic pathway activation in breast carcinoma patients	[295]
^{99m}Tc-N_2S_2-Annexin V	Acute cardiac transplant rejection patients	[135, 136]
^{99m}Tc-N_2S_2-Annexin V	AMI patients	[296]
^{99m}Tc-N_2S_2-Annexin V	Biodistribution and dosimetry study in patients with sub-acute MI, heart failure, non-Hodgkin's lymphoma and Hodgkin's disease	[137]
^{99m}Tc-N_2S_2-Annexin V	Chemotherapy-induced apoptosis in lung and breast cancer and lymphoma patients	[35]
^{99m}Tc-N_2S_2-Annexin V	Follicular lymphoma patients receiving radiotherapy	[139]
^{99m}Tc-N_2S_2-Annexin V	Intracardiac tumour case report	[70]
^{99m}Tc-N_2S_2-Annexin V	NSCLC patients receiving platinum-based chemotherapy	[138]

(A)MI, (Acute) myocardial infarction; IP, ischaemic preconditioning; MRI, magnetic resonance imaging; NSCLC, non-small cell lung cancer

At the beginning of 2002, ^{99m}Tc-Hynic-Annexin V entered phase I clinical trials to determine the safety, biodistribution and dosimetry of the molecule prior to clinical use in nuclear medicine [146]. Similar to the penthioate radioligand, ^{99m}Tc-Hynic-Annexin V showed strongest uptake in the kidneys, liver and urine bladder on early patient images. However, activity uptake in liver and kidneys was significantly higher (i.e. by a factor of 2–2.5 and 6–13, respectively) for both ^{99m}Tc-Annexin V ligands compared with ^{123}I-Annexin V. Like the iodinated protein, ^{99m}Tc-Hynic-Annexin V generally showed predominantly urinary excretion. Nevertheless, the total % injected dose found excreted in urine remained substantially lower than that observed with ^{99m}Tc-BTAP-Anx V (i.e. 22.5%±3.5% ID vs 65%±11% ID at 20–24 h p.i.). Furthermore, the biodistribution of ^{99m}Tc-Hynic-Annexin was devoid of any bowel excretion, resulting in excellent imaging conditions in the abdominal region. Regardless of the applied radiolabelling method, both the ^{99m}Tc-Annexin V radioligands and ^{123}I-rh-Annexin V generally exhibit a rapid, bi-exponential clearance from the blood circulation, although some differences do exist between the agents. Respectively 92%, 87% and 74% of the ^{99m}Tc-Hynic-, ^{99m}Tc-N_2S_2- and ^{123}I-Annexin V activity is cleared from the blood in a fast phase with a $T_{1/2,\alpha}$=24, 26 and 4 min whereas the remaining blood pool activity is slowly excreted with a $T_{1/2,\beta}$=35, 6.9 and 4.1 h). From a dosimetry point of view, for ^{99m}Tc-Annexin V radioligands, the organs receiving the highest absorbed dose are kidneys, spleen and liver. However, in the case of ^{123}I-rh-Annexin V, the absorbed dose to the kidneys and spleen was much lower whereas the absorbed dose to liver was comparable. Red bone marrow and urine bladder also received similar absorbed doses. In contrast, the high thyroid uptake observed for ^{123}I-rh-Annexin V resulted in an 11- to 14-fold increase in the absorbed dose in comparison with ^{99m}Tc-labelled Annexin V. Furthermore, administration of ^{123}I-rh-Annexin V to human subjects resulted in an effective dose about twofold higher than that reported for the ^{99m}Tc-Annexin V radioligands.

Soon afterwards, phase I human studies were initiated with the most prominent clinical applications comprising in vivo detection of myocardial infarction [147–149], intracardiac tumours and infectious endocarditis [150] and spontaneous as well as chemotherapy- or radiotherapy-induced apoptosis in a variety of solid and haematological tumours [138, 139, 151, 152]. In this regard, systematic radionuclide detection of apoptosis during the course of tumour therapy would not only enable physicians to monitor the efficacy of treatment over time and patient outcome, but would also allow early prediction of therapy response, thereby avoiding unnecessary and time-consuming treatment courses. At present, ^{99m}Tc-Hynic-Annexin V is the only apoptosis-detecting radioligand that is currently being investigated in phase II/III trials in patients with non-small-cell lung cancer [138] and is likely to reach the stage of commercialisation for routine use in nuclear medicine.

^{99m}Tc-i-Annexin V. In the follow-up of ^{99m}Tc-BTAP-Anx V, a third type of ^{99m}Tc-Annexin V was developed and evaluated soon afterwards in human subjects [153]. Annexin V was derivatised with a monodentate *n*-1-imino-4-mercaptobutyryl side chain and subsequently labelled with ^{99m}Tc based on the earlier reported method of Goedemans and Panck [154]. The iminothiolane approach consists of converting amino groups within the protein into free thiol groups which can readily bind to ^{99m}Tc in the presence of stannous ions. Although this labelling method allowed fast and easy preparation of ^{99m}Tc-(*n*-1-imino-4-mercapto-butyl)-Annexin V (^{99m}Tc-i-Anx V, Mallinckrodt, Petten, The Netherlands), only low radiochemical purities of 79–82% could be obtained, making it less suitable for common use in clinical settings.

Biodistribution studies in human subjects injected with this iminothiolane preparation gave results for the most vital organs that were similar to those obtained with ^{99m}Tc-BTAP-Anx V. However, with the exception of the urinary bladder and large intestine wall, the absorbed radiation doses for most organs were higher in the case of ^{99m}Tc-i-Anx V owing to its substantial longer effective biological half-life in the total body (i.e. 62±13 h vs 16±7 h for ^{99m}Tc-BTAP-Anx V). Thus, ^{99m}Tc-i-Anx V seemed to be subject to slower clearance from most organs, resulting in two- to threefold higher radiation doses to the urinary bladder and large intestine wall. These findings were clearly reflected by slower clearance from the blood and less pronounced radioactivity accumulation in the bowels, as previously observed with ^{99m}Tc-BTAP-Anx V. Nevertheless, the radiopharmaceutical was applied successfully in patients with AMI who were receiving reperfusion therapy. Following 2 h of reperfusion, the infarcted area of the heart could be clearly detected on late SPECT images 17–22 h after tracer injection [69]. In contrast, increased radioligand uptake was seen neither in the heart outside the infarcted area nor in the heart of a control patient. Perfusion scintigraphy with sestamibi 6–8 weeks later demonstrated co-localisation of an irreversible perfusion defect with the area of increased ^{99m}Tc-i-Anx V uptake. However, on early SPECT images (i.e. 3–4 h p.i.), visualisation of myocardial tracer uptake was significantly hampered by the high blood pool activity. These findings indicate that reperfusion is associated with irreversible cell death in infarcted cardiac tissue and confirm previous studies which demonstrated the involvement of both apoptotic and oncotic cell death in myocardial ischaemia and reperfusion [63, 155].

^{99m}Tc-MAG$_3$-Annexin V. In an effort to decrease the high kidney and liver accumulation observed for most ^{99m}Tc-labelled Annexin V compounds, in particular ^{99m}Tc-Hynic-Annexin V, the protein was recently conjugated to mercaptoacetyl-glycyl-glycine (MAG$_3$) [156]. In fact, the MAG$_3$ chelator has been applied in the ^{99m}Tc chemistry of proteins and peptides many fold, often resulting in good renal clearance. Similar to the Hynic post-labelling methodology, NHS-MAG$_3$ can be attached to Annexin V at room temperature in a single step. Radiolabelling of the purified N_3S chelate resulted in radiochemical yields of 90% under basic pH conditions, eliminating the need for further purification on a column. Preliminary biodistribution data in mice clearly showed significant decreases (by 62.8% and 52.6%, respectively) in the kidney and liver uptake of ^{99m}Tc-MAG$_3$-Annexin V at 1 h p.i. compared with ^{99m}Tc-Hynic-Annexin V. Ongoing biodistribution studies in mice indicate an even more pronounced decrease in liver uptake of 84.6% (no results shown). Furthermore, the ^{99m}Tc-MAG$_3$-Annexin V biodistribution was characterised by lower retention of radioactivity in the whole body whereas blood and intestinal uptake was threefold higher than that observed with ^{99m}Tc-Hynic-Annexin V. However, ongoing studies have revealed a sixfold higher tracer uptake in the small intestines for the MAG$_3$ derivative at 1 h p.i., with blood pool activity being almost 1.4-fold lower than that of ^{99m}Tc-Hynic-Annexin V. These findings seem to confirm the expected improvement in renal and hepatic clearance of the MAG$_3$ radioligand, which could at least contribute to better imaging conditions for the study of apoptosis in kidney diseases. However, early in vivo detection of ongoing apoptosis in the liver might be hampered by the significantly increased activity uptake in the small intestines despite the improved hepatic clearance of ^{99m}Tc-MAG$_3$-Annexin V.

^{94m}Tc-Hynic-Annexin V. Very recently a technetium-based PET alternative to ^{99m}Tc-Hynic-Annexin V was studied by McQuade et al., applying ^{94m}Tc as the radionuclide [157]. Given the unique radionuclidic properties of this isotope (physical half-life of ^{94m}Tc=53 min, $E_{max}\beta^+$=2.5 MeV), ^{94m}Tc-Hynic-Annexin V could be considered a valuable marker for in vivo detection of apoptosis by means of PET. Since ^{94m}Tc and ^{99m}Tc share identical physicochemical properties, ^{94m}Tc-Hynic-Annexin V can be produced using the same methodology as its SPECT counterpart, resulting in comparable radiochemical yields and purities >90%. Considering the superior resolution of PET over SPECT, positron-emitting apoptosis-detecting ligands seem very attractive, especially in cases where the ongoing apoptotic process is localised in small tissue areas (e.g. tumour nodules or focal ischaemic tissue zones) or in the presence of a weak apoptotic signal (e.g. subacute myocarditis). At present, ^{94m}Tc-Hynic-Annexin V is being evaluated in a mice model of anti-Fas MoAb-induced hepatic apoptosis [157].

^{99m}Tc-EDDA-Hynexin. In addition to tricine, several alternative co-ligands such as *N*,*N*-ethylenediamine diacetic acid (EDDA), tricine/nicotinic acid or isonicotinic acid can be considered for the ^{99m}Tc-labelling of Hynic-

Annexin V. The choice of co-ligand not only determines the number of possible isomers but also affects the lipophilic properties, in vivo stability and subsequent biological behaviour of the corresponding Hynic-technetium complexes [158].

In a study published by Verbeke et al., EDDA was used as co-ligand for labelling Hynic-derivatised Annexin V (Fig. 3B) [159]. Conjugation of the Hynic chelator to Annexin V and radiolabelling of the conjugate were performed similarly to the standard methods as described above. However, in contrast to the tricine-based preparations performed at room temperature, reaction mixtures for ^{99m}Tc labelling of EDDA-Hynexin required incubation at 37°C. Despite the heating process, poor radiochemical yields were obtained for ^{99m}Tc-EDDA-Hynexin (i.e. 28% and 35% after 20 and 60 min incubation time, respectively), whereas ^{99m}Tc-Hynic-Annexin V is consistently produced in radiochemical yields >90%. As a result, ^{99m}Tc-EDDA-Hynexin preparations require an extra purification step (e.g. by means of size-exclusion FPLC) in order to achieve adequate radiochemical purity prior to administration in animals. Biodistribution studies with ^{99m}Tc-EDDA-Hynexin in mice demonstrated a fairly rapid blood clearance and predominant uptake in kidneys and liver, as previously observed with ^{99m}Tc-Hynic-Annexin V. However, radioactivity accumulation in kidneys was significantly higher for ^{99m}Tc-EDDA-Hynexin, while liver uptake was much lower compared with that of ^{99m}Tc-Hynic-Annexin V. Furthermore, the two radioligands exhibited comparable, low urinary excretion 60 min after administration [160]. These findings could be explained by the lower lipophilicity of the EDDA co-ligand in comparison with tricine since decreased lipophilicity of co-ligands results in decreasingly lipophilic ^{99m}Tc-Hynic complexes which are generally known to provide lower abdominal excretion and organ uptake, particularly in the liver, followed by a higher renal excretion [158]. Nevertheless, the EDDA co-ligand does not appear to be a suitable alternative to tricine in the routine production of ^{99m}Tc-Hynic-Annexin V, considering the very low radiochemical yields.

^{99m}Tc-EC-Annexin V. An alternative method for preparing ^{99m}Tc-rh-Annexin V was described by Yang and Kim et al. making use of ethylenedicysteine (EC) as a bifunctional chelating agent. ^{99m}Tc-EC-Annexin V was produced by conjugation of EC to the protein, applying sulpho-*N*-hydroxysuccinimide (sulpho-NHS) and 1-ethyl-3-[3-(dimethylamino)propyl]-carbodiimide-HCl (EDC) as coupling agents [161, 162]. In a second step, the ethylene cysteine construct was radiolabelled with ^{99m}Tc and $SnCl_2$ followed by purification through gel permeation, which resulted in overall radiochemical yields of 65–70% and purities near 100%. Furthermore, ^{99m}Tc-EC-Annexin V could be obtained in high specific activities of 185 GBq/μmol. In fact, radiopharmaceutical preparation of ^{99m}Tc-EC-Annexin V was based on the N_2S_2 bifunctional chelate approach, similar to preparation of the renal imaging agent ^{99m}Tc-EC, which is characterised by easy and efficient radiolabelling providing high radiochemical purity and stability. Although ^{99m}Tc-EC-Annexin V does not require any co-ligand for stabilising the radioligand, an additional purification step is necessary to obtain a sufficient radiochemical purity above 95%.

When evaluated in different animal models of spontaneous tumour apoptosis, highly apoptotic ovarian and breast tumour-bearing rodents showed moderate to high tumour radioligand uptake peaking within 15 min to 2 h post radioligand injection, after which the signal already started to decrease. These results seem to reflect an undesirable rapid tumour clearance of the tracer; this could be detrimental for clinical use of the tracer in nuclear medicine, which requires apoptosis imaging over longer periods (i.e. 6–24 h p.i.). Additionally, the specificity of the radioactivity uptake in the investigated tumours was unclear since ^{99m}Tc-L,L-ethylenedicysteine (^{99m}Tc-EC) was used as the control radioligand in these studies. Nevertheless, ^{99m}Tc-EC-metronidazole scintigraphic images in the same breast tumour-bearing rodents suggested a co-localisation of the area of tumour hypoxia with ongoing apoptosis, indicating the presence of hypoxia-induced apoptosis. In contrast, virtually no ^{99m}Tc-EC-Annexin V uptake could be documented in low apoptotic sarcomas within the same time frame.

Additional planar imaging studies were performed with implanted rat breast cancer tumours, which were treated with either paclitaxel or irradiation [162, 163]. Significantly increased tracer uptake was only observed in tumours 3 days after paclitaxel treatment; by contrast, tumour uptake was slightly lower at 5 days post therapy when compared with pre-therapy planar rat images. Furthermore, the overall tumour uptake of ^{99m}Tc-EC-Annexin V in paclitaxel-treated rats (i.e. 0.2–0.5% ID/g) within 0.5–4 h after tracer injection was rather low, resulting in poor tumour-to-blood ratios of 0.4–0.8. Considering the generally rapid clearance of apoptotic cells in vivo, early detection of chemo- or radiotherapy-induced apoptosis within 24 h post treatment would seem more likely to result in higher tumour-to-background ratios when the apoptotic tumour cells have not yet been extensively removed by macrophages and neighbouring cells. Indeed, several in vitro and in vivo studies have clearly demonstrated that a substantial rise in tumour cell apoptosis can occur within or around 24 h following chemotherapy or radiotherapy treatment [87, 164–166]. Again, these findings seem to confirm the necessity of determining the timing of PS exposure when studying chemotherapy- or radiotherapy-induced apoptosis in vivo.

Directly labelled ^{99m}Tc-Annexin V. In pursuit of a fast and simple method for ^{99m}Tc labelling of Annexin V, Zhu et al. recently described a direct labelling approach

in which the free thiol group of the protein was reduced in the presence of Sn^{2+} ions and citrate [167]. Reaction times of merely 10 min resulted in high radiochemical yields and purities above 95%, whereas the radioligand showed adequate in vitro stability at 10 h post labelling.

As previously reported in the literature, the direct ^{99m}Tc-labelling approach offers a quick and easy method for producing ^{99m}Tc-labelled antibodies and smaller proteins with high radiochemical yields and stability, often without requiring any additional purification steps. Subsequently, ^{99m}Tc complexation by reduced sulph-hydryl groups and free NH_2 groups is supposed to result in N_2S_2 chelates whose radiochemical stability and biological activity greatly depend on the density of the thiol groups within the protein [168]. Considering the variety of amino acids involved in this type of chelation along with their complex location in the protein's structure, it remains difficult to predict the aforementioned characteristics. Since Annexin V exhibits only one cysteine residue buried within its tertiary structure, this approach is likely to generate a tracer with low specific activity, thereby making it less attractive for in vivo application. Thus, the preliminary data on directly ^{99m}Tc-labelled Annexin V require further evaluation in order to fully confirm the reproducibility of the radiolabelling method as well as the biopotency of the molecule.

^{99m}Tc-SDH-Annexin V. In addition to direct ^{99m}Tc-labelling of Annexin V, a second simplified method was suggested by Subbarayan et al., also making use of a single reaction step [169]. In this pre-formed chelate approach, ^{99m}Tc was sequestered first by using succinic dihydrazide (SDH) along with tricine and nicotinic acid, after which the chelate was conjugated to the protein by heating at 90°C. The obtained radiochemical yield and purity both exceeded 95% initially, while 94% of ^{99m}Tc-SDH-Annexin V was recovered in saline and plasma 24 h post radiolabelling. Although Subbarayan et al. postulated that ^{99m}Tc-SDH-Annexin V production was significantly simpler than ^{99m}Tc labelling of Hynic-Annexin V, both types of kit preparation consist of one reaction step (i.e. starting from two kit vials) which provide comparable high radiochemical yields and purities, excluding any additional purification steps. However, the ^{99m}Tc-SDH-Annexin V radiolabelling requires extensive heating at 90°C for 10 min, which makes it less attractive for routine clinical use. Furthermore, it is very unlikely that the protein remains structurally intact at such a high reaction temperature. Previous studies have clearly demonstrated that many proteins, and Annexin V in particular, are very sensitive to elevated temperatures, which cause progressive denaturation and subsequent loss in biological activity. Moreover, some studies have even used heat-inactivated Annexin V as a negative control in ex vivo Annexin V binding assays. In such cases, heating at 56°C for 10 min was already sufficient to yield complete inactivation of the protein [90, 170]. These considerations could explain the apparent excellent stability of ^{99m}Tc-SDH-Annexin V in plasma compared with the in vitro stability in saline, since the protein has already been denaturated during radiolabelling, thereby making it virtually resistant to any further enzymatic breakdown in plasma. PD-10 size exclusion chromatography also revealed a clearly different elution profile of ^{99m}Tc-SDH-Annexin V compared with unlabelled Annexin V, indicating a discordance between the products' identities. In addition, HPLC analysis of the radioligand indicated two significant shoulder peaks, which were not identified.

All these findings raise serious doubts over the identity and radiopharmaceutical quality of ^{99m}Tc-SDH-Annexin V and over the relevance of the first biopotency data obtained in vitro [171] and in vivo in a tumour mice model of photodynamic therapy-induced apoptosis [169].

^{99m}Tc-Annexin V mutants. At the beginning of the 1990s, Huber et al. were the first to succeed in revealing the crystal and molecular structure of human Annexin V [52, 53, 172]. However, very soon afterwards the first mutant forms of the recombinant protein were developed by Tait et al. in order to study the structural basis for the high-affinity Annexin V membrane binding. Since His-204 and its adjacent residues in the third repeat of Annexin V (i.e. Arg-200, Arg-206 and Lys-207) were believed to be essential for anticoagulant activity, site-specific mutagenesis of basic residues in this region by alanine seemed a promising approach for constructing short Annexin V derivatised peptides with increased anticoagulant properties [173]. Furthermore, such peptides, when radiolabelled, might prove most valuable as thrombus-detecting agents. Unfortunately, the produced 200A, 204A, 206A and 207A mutants exhibited unchanged binding affinity to phospholipids compared with the wild-type protein, indicating that the anticoagulant activity for short peptide sequences corresponding to this region was not related to their structural resemblance to the phospholipid binding region of unmodified Annexin V.

In pursuit of identifying new PS-recognising sites in Annexin V and studying their involvement in Ca^{2+}-dependent membrane binding and their inhibitory effect on cytosolic phospholipase A_2 ($cPLA_2$) activation, several in depth studies were published more recently by the group of Russo-Marie et al. on a second group of Annexin V mutants [174, 175]. Based on the initial structure analyses of Huber et al., three high-affinity Ca^{2+}-binding sites (i.e. Glu-72, Asp-144, Asp-303) had been identified in the domains I, II and IV of Annexin V. However, a fourth less essential Ca^{2+}-binding site (i.e. Glu-228) was discovered in domain III and appeared to be related to the presence of the Trp-186 and Trp-187 residues, which are located near the membrane surface in the Annexin V-phospholipid complex [176, 177]. Subsequent mutagenesis (i.e. Glu Gln or Ala, Asp Asn) of one

or more of these amino acids responsible for the bidentate attachment of calcium resulted in a class of single and multiple mutant constructs with different PS-binding properties and inhibitory effects on $cPLA_2$ activity. Of special interest were the quadruple mutant M1M2M3M4, containing all four defective Ca^{2+}-binding sites (i.e. bearing one mutation in each Annexin V domain), and the M1M2M4 mutant, which had both completely lost their inhibitory effect on $cPLA_2$ activation in comparison with wild-type recombinant Annexin V. These mutant proteins revealed that the Ca^{2+}-binding site located in domain I of Annexin V plays a major role in the inhibition of $cPLA_2$ activity, whereas the fourth site is of secondary importance. In contrast, the Ca^{2+} sites located in domains II and III did not participate in this process while their overall molecular structure, as for the other mutants, was basically unaltered compared with the recombinant wild-type protein. Similar results were found when studying the inhibitory effect of wild-type and mutant Annexin V on cytosolic protein kinase C activity [178]. Additionally, enhanced mutational analysis in domain I of the M2M3M4 mutant has recently revealed a new PS-binding site which corresponds to a highly conserved consensus sequence present in the complete Annexin family [175].

Anyhow, the quadruple mutant M1M2M3M4 construct that became available through the increase in mutational analysis studies proved to be most suitable as a control protein for demonstrating the specificity of (wild-type) Annexin V binding to apoptotic cells or activated blood platelets. An increasing number of preclinical ^{99m}Tc-Hynic-Annexin V studies have started to use ^{99m}Tc-labelled M1M2M3M4 Annexin V as the control radioligand rather than radiolabelled human serum albumin, which has generally been used as a control protein in nuclear medicine for many years. Since M1M2M3M4 Annexin V possesses a very comparable molecular weight to wild-type Annexin V (MW 35,744 and 35,935, respectively), with a virtually unmodified overall molecular structure and only slight changes in physicochemical properties, it is probably the best control protein at present for demonstrating the specific nature of Annexin V binding.

Moreover, a new type of Annexin V mutant was recently developed by Tait et al. which carries an endogenous chelation site for ^{99m}Tc, thereby allowing direct ^{99m}Tc labelling of the protein [179]. The three mutant molecules, designated Annexin V-116, V-117 and V-118, were constructed by introducing seven amino acid sequences (i.e. containing either one or two cysteine residues) to the N-terminal side of Annexin V, whereas the naturally occurring Cys-316 was mutated to Ser in all three proteins (Fig. 4). Although radiolabelling of the mutant molecules was based on a simplified version of the method previously described for the ^{99m}Tc-N_2S_2-Annexin V, much higher radiochemical yields and purities were achieved while the overall reaction times were much smaller. This approach resulted in high specific activities of at least 66–132 GBq/μmol (i.e. especially for Annexin V-117 and Annexin V-118), which are more comparable with that of ^{99m}Tc-Hynic-Annexin V, while all radiolabelled mutants showed favourable in vitro stabilities over time. Both the non-radiolabelled and the ^{99m}Tc-labelled mutants demonstrated a fully preserved biological activity compared with Hynic-Annexin V and ^{99m}Tc-Hynic-Annexin V, respectively. Likewise, biodistribution studies in mice revealed predominant uptake in liver and kidneys for all radiolabelled mutants (ranging from 5.9% to 11.2% ID and from 5.9% to 17.9% ID, respectively), although the extent of uptake in these organs, along with spleen and bone marrow uptake, was significantly decreased in comparison with ^{99m}Tc-Hynic-Annexin V uptake (i.e. 16.6% ID and 39.1% ID for liver and kidney, respectively). In contrast, the abdominal clearance of the radiolabelled mutants was moderately increased [180–182]. Since Annexin V-116 and Annexin V-117 were assumed to form N_3S chelates whereas Annexin V-118 was believed to generate an N_2S_2 chelate, it seems conceivable that these chelates resulted in a somewhat higher abdominal uptake, albeit much less pronounced than that previously observed with the ^{99m}Tc-N_2S_2-Annexin V. Annexin V-117, which showed the most beneficial overall biodistribution properties, was further evaluated in a rat model of intramedullary cyclophosphamide-induced apoptosis. Significantly increased uptake was confirmed in femur and spleen 24 h post treatment due to ongoing apoptosis in bone marrow cells and splenocytes. In addition, cyclophosphamide-

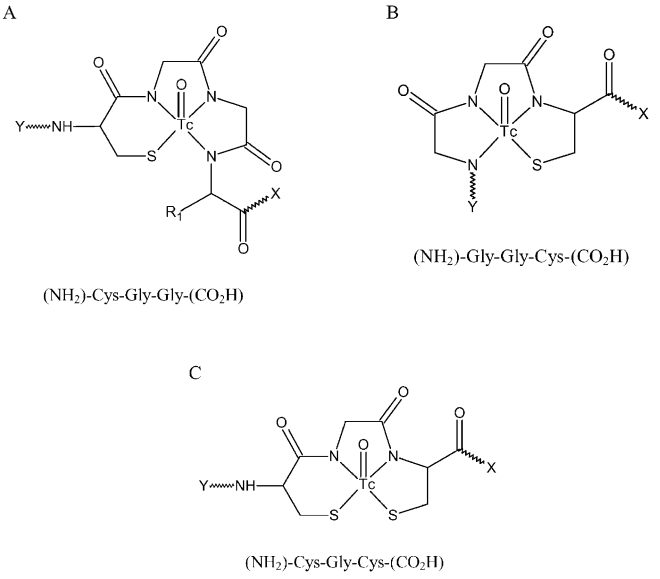

Fig. 4A–C. Chemical structure of ^{99m}Tc-labelled Annexin V mutant molecules with endogenous chelation sites: **A** ^{99m}Tc-Annexin V-116, **B** ^{99m}Tc-Annexin V-117, **C** ^{99m}Tc-Annexin V-118. Y and X respectively represent the amino and carboxy terminal ends of the mutated Annexin V sequence

Table 3. Primary structures of Annexin V mutants. Each mutant protein contains the indicated N-terminal sequence (italicised) followed by the amino acids 2–320 of human Annexin V. The initiator Met residue is removed post-translationally from all mutant proteins and therefore not shown. In the Annexin V mutants 116, 117 and 118, the naturally occurring Cys residue at position 316 has also been mutated to Ser

Protein name	N-terminal sequence	IC_{50} (n*M*)[a]	Radiochemical yield[b] (%)	Radiochemical purity[b] (%)	Erythrocyte binding[c] (%)
Annexin V-wt[d]	NH_2-Ala-Gln-Val ···	9.0±4.0	43.0±3.9	91.2±1.7	78.3[e]
Annexin V-wt	NH_2-Ala-Gln-Val ···	6.8±0.7	3.9±1.6	NA	NA
Annexin V-116	NH_2-*Ala-Cys-Gly-Gly-Gly-His-Met-* ···	9.3±0.4	89.5±5.7	94.4±2.0	77.5±3.5
Annexin V-117	NH_2-*Ala-Gly-Gly-Cys-Gly-His-Met-* ···	10.3±2.5	88.8±2.0	92.2±1.2	78.1±3.8
Annexin V-118	NH_2-*Ala-Cys-Gly-Cys-Gly-His-Met-* ···	10.0±2.8	89.9±1.9	94.2±0.6	78.7±3.6
Annexin V-122[d]	NH_2-*Ala-His-His-His*-Ala-Gln-Val- ···	7.0±1.0	60.6±6.4	96.7±0.9	80.7±0.9
Annexin V-123[d]	NH_2-*Ala-His-His-His-His-His-His*-Ala-Gln-Val ···	6.0±2.0	80.6±0.6	98.4±0.5	85.0±2.8
Hynic-Annexin V	10.1±2.0	97.0[e]	99.0[e]	83.9±2.5	

All presented data were adapted from Tait et al. [179, 185]
wt, Wild-type; NA, not applicable
[a] Membrane binding activity of unlabelled mutant Annexin V proteins. IC_{50} values for the mutant proteins were determined by a competition assay with FITC-Annexin V for binding to erythrocytes
[b] Radiochemical yield and radiochemical purity (i.e. after purification by gel filtration) as determined by ITLC
[c] Membrane binding activity of ^{99m}Tc-labelled mutant Annexin V proteins. Binding to erythrocytes was determined similarly to the method described for the unlabelled mutant proteins
[d] Results from the tricarbonyl radiolabelling method
[e] Data originating from single measurements

treated mice showed substantially elevated tracer accumulation in the heart, spleen and bowels as early as 6 h post therapy. These results seem to suggest that ^{99m}Tc-Annexin V-117, owing to its lower basal overall uptake in healthy organs, might provide even higher target-to-background ratios than ^{99m}Tc-Hynic-Annexin V when imaging chemotherapy-induced apoptosis [180–182]. Nevertheless, the absolute tumour uptake of ^{99m}Tc-Annexin V-117 in cyclophosphamide-treated KDH-8 hepatomas reported by Kuge et al. [183] was threefold lower compared with earlier reported data for ^{99m}Tc-Hynic-Annexin V in the same rat model [184].

Soon afterwards, another class of Annexin V mutants emerged which was specifically designed to allow radiolabelling by means of the tricarbonyl $^{99m}Tc(CO)_3$ core [185]. For this purpose, N-terminal extentions containing either three or six histidine (His) residues were attached to the protein since His is known to form highly stable multivalent complexes with $[^{99m}Tc(CO)_3(H_2O)_3]^+$, thereby resulting in high specific activities. Similar to the previously described molecules, mutant forms of human Annexin V cDNA were cloned in an expression vector and expressed cytoplasmaticaly in *E. coli*, after which they were purified in high yields and purity. $^{99m}Tc(CO)_3$ labelling of the Annexin V-122 and Annexin V-123 mutants resulted in similar radiochemical yields, in vitro stability and biopotencies as were observed for the mutants bearing endogenous chelation sites (Table 3). Although Annexin V-123 exhibited the most advantageous overall radiochemical properties, specific activies (i.e. at least 13–26 GBq/µmol) were nevertheless considerably lower compared with those reported for ^{99m}Tc-Annexin V-116, -117 and -118 mutants. Although less complex and time-consuming than the multistep N_2S_2 method, tricarbonyl labelling of His-tagged proteins still requires a two-step procedure in which the $[^{99m}Tc(CO)_3(H_2O)_3]^+$ chelate must be first formed in a separate step at 100°C. In contrast, recombinant proteins with endogenous chelation sites (i.e. in particular Annexin V-117), like Hynic-Annexin V, can be used for direct ^{99m}Tc labelling at room temperature or 37°C and therefore provide a faster and more simple labelling method for routine production in a clinical setting.

^{99m}Tc-tricarbonyl Annexin V. As with the above-mentioned Annexin V-122 and Annexin V-123 mutants, $^{99m}Tc(CO)_3$ labelling has also been applied to native Annexin V by two different methods. In an effort to address the generally observed high renal and hepatic accumulation of ^{99m}Tc-labelled Annexin V, Han et al. developed the tricarbonyl ligand [$^{99m}Tc(CO)_3$ PADA]-AV based on the previously established method of Alberto et al. [186]. For this purpose, $[^{99m}Tc(CO)_3(H_2O)_3]^+$ was complexed with picolylamine-*N*,*N*-diacetic acid (PADA), after which the pre-formed chelate was converted to an activated trifluorophenyl (TFP) ester and conjugated to Annexin V [187]. As reflected by in vitro stability experiments, tricarbonyl labelling of PADA resulted in a stable complex remaining fully intact at 16 h of excessive histidine challenge. Subsequently, [$^{99m}Tc(CO)_3$ PADA]-AV exhibited fast uptake in kidneys, liver and spleen of mice early after administration (i.e. 78%, 36% and 31% ID/g at 0.25 h p.i., respectively), followed by a gradual clearance over time with, respectively, 2%, 3% and 2% remaining at 12 h p.i. Although lower early activity uptake was reported in all these organs for ^{99m}Tc-Hynic-

Annexin V [141, 188, 189], the kidney accumulation of [^{99m}Tc(CO)$_3$ PADA]-AV at 3 h p.i. was already significantly lower whereas liver and spleen uptake remained slightly higher. Considering this finding in conjunction with a very fast blood clearance and low residual body retention, [^{99m}Tc(CO)$_3$ PADA]-AV seems to be characterised by improved pharmacokinetic properties.

A second tricarbonyl method recently emerged which was applied to Hynic-derivatised DNA analogues [190] and proteins like Annexin V [191]. Since the Hynic chelator has been shown to sequester the ^{99m}Tc(I) tricarbonyl ion easily, [^{99m}Tc(CO)$_3$(H$_2$O)$_3$]$^+$ was coupled to Hynic-Annexin V in a single reaction step, yielding radiochemical purities of about 90% after additional purification. Preliminary biodistribution studies in Balb/c mice with anti-Fas MoAb-induced hepatic apoptosis showed predominant activity retention in liver and kidneys. Furthermore, the twofold increase in hepatic uptake of ^{99m}Tc(I)-Hynic-Annexin V compared with control animals was in the same order of magnitude as that observed with conventional ^{99m}Tc-Hynic-Annexin in 1 h-treated Balb/c mice as reported by Blankenberg et al. [141]. Therefore, ^{99m}Tc(I)-Hynic-Annexin V seems to hold potential for in vivo monitoring of apoptosis. However, in spite of the easy and kinetically fast complexation of [^{99m}Tc(CO)$_3$(H$_2$O)$_3$]$^+$ to Hynic-Annexin V, the tricarbonyl approach provides a less stable radioligand compared with ^{99m}Tc (V)O^{3+}-labelled Hynic-Annexin V since only 70% of the molecule remains intact in saline or plasma 4 h after preparation. In this regard, the ^{99m}Tc-Hynic-Annexin V as originally developed by Blankenberg et al., based on the method of Abrams et al., remains a better choice of radioligand [140, 141].

^{111}Indium-DTPA-PEG-Annexin V

Following the initiation, execution and disintegration phases of the apoptotic cell death process, the remaining small "apoptotic bodies" will finally be recognised by macrophages and neighbouring cells which will engulf and eliminate the cell fragments by phagocytosis. Thus, externalisation of PS residues to the surface of dying cells eventually acts as a "removal" signal for macrophages which express the PS receptor. Concordantly, apoptotic cell death represents a dynamic process, which provides a temporary time frame for detection in vivo. In this context, apoptosis-detecting radioligands with a prolonged circulation in the blood compartment in theory might provide improved visualisation conditions for apoptosis detection in tumours. In search of such apoptosis markers with enhanced imaging properties, Li et al. developed a PEGylated Annexin V construct in order to increase the biological half-life of the protein [192]. Polyethyleneglycol (PEG) was used as a spacer between Annexin V and diethylene triamine penta-acetic acid (DTPA) as the chelating group, after which the molecule was radiolabelled with ^{111}In. ^{111}In-DTPA-PEG-Annexin V could be obtained in high radiochemical yields (i.e. 92%) with excellent radiochemical purity of >98%.

^{111}In-DTPA-PEG-Annexin V was also evaluated in a tumour model of paclitaxel and anti-EGR MoAb-induced apoptosis in mammary MDA-MB468 tumour-bearing nude mice. Paclitaxel-treated animals showed significantly increased tumour uptake 4 days post treatment, whereas a substantial decrease in radioligand tumour uptake was seen in nude mice treated with the anti-EGR MoAb. In addition, a good correlation was found between the radioligand uptake in tumours and the apoptotic index determined histologically (r^2=0.77). Whole-body gamma images of treated nude mice at 48 h following tracer injection clearly demonstrated an enhancement of the contrast in the tumours, thereby providing first evidence for the hypothesis that a prolonged circulation of radiolabelled Annexin V in the body might contribute to improved visualisation of tumour apoptosis. In this regard, the ^{111}In radionuclide seems a good choice for diagnostic imaging of apoptosis, considering its prolonged half-life (physical half-life of ^{111}In=2.81 days, $E_{max}\gamma$=0.172, 0.247 MeV) and relatively low gamma energies.

^{11}Carbon-Annexin V

Another radioligand for PET imaging of apoptosis was proposed by Ito et al., who introduced ^{11}C (physical half-life of ^{11}C=20.39 min, $E_{max}\beta^+$=0.961 MeV) into the Annexin V protein [193]. In a first step, $^{11}CH_3I$ was generated from the cyclotron product $^{11}CO_2$ through autochemical synthesis. Afterwards $^{11}CH_3I$ was reacted with Annexin V dissolved in an MeOH solution at –20°C. The reaction was allowed to proceed for 5 min at 80°C, followed by solvent dry out under vacuum and reconstitution of the newly formed ^{11}C-Annexin V in saline. Radiochemical yields were in the range 10–15% with an RCP above 95% as determined by HPLC. The biopotency of ^{11}C-Annexin V was tested in vitro towards Gc-4SD cells (5% apoptotic) and Gc-4PF cells (34% apoptotic). Although the Gc-4PF cells were reported to show significantly increased tracer uptake over Gc-4SD cells, no data were provided to support these findings or to demonstrate the specificity of the radioligand uptake.

Furthermore, ^{11}C-labelled Annexin V does not seem to be a suitable PET ligand for imaging cell death for several reasons: The physical half-life of ^{11}C will undoubtedly be too short to allow repeated in vivo monitoring of the apoptotic process over time, thereby severely reducing the time window for detection almost to a single moment. As a result, much crucial information will be lost concerning the kinetics of the biological process. Secondly, the radiolabelling procedure for preparing ^{11}C-Annexin V on a routine basis is rather complicated and time-consuming. In particular, the very poor radio-

chemical yields associated with the production of short-living ^{11}C-Annexin V represent a major constraint for the clinical applicability of the radioligand. Most importantly, ^{11}C-labelling of Annexin V requires an extensive heating step similar to that described for ^{99m}Tc-SDH-Annexin V, which should result in substantial denaturation of the protein and a subsequent loss in biological activity. In this regard, alternative approaches for the proposed radiolabelling of ^{11}C-Annexin V seem mandatory.

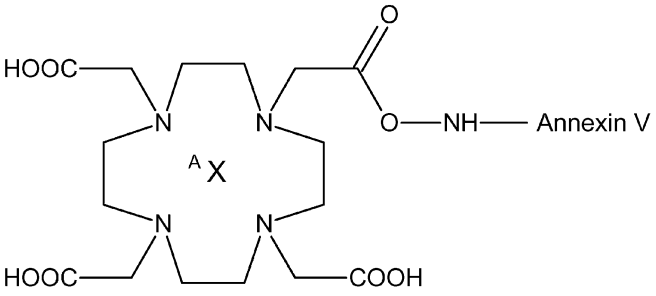

Fig. 5. Chemical structure of DOTA-Annexin V with ^{A}X=^{64}Cu, ^{67}Ga or ^{68}Ga

^{64}Cu-DOTA-Annexin V

Along with ^{94m}Tc-Hynic-Annexin V, a new Annexin V-based PET ligand recently emerged which was actually developed by the same research group. McQuade et al. reported on the radiolabelling of DOTA-conjugated Annexin V with ^{64}Cu as an alternative PET radionuclide [157]. For this purpose, 1,4,7,10-tetraazacyclododecane-*N*,*N*′,*N*″,*N*‴-tetra-acetic acid (DOTA) was first activated with 1-ethyl-3-[3-(dimethylamino)propyl]-carbodiimide (EDC) and *N*-hydroxy sulphosuccinimide (sulpho-NHS) and afterwards conjugated to Annexin V. In a third step, DOTA-Annexin V was reacted with ^{64}Cu under heating at 55°C for 40 min, which resulted in high specific activities (i.e. 106–132 GBq/μmol) and radiochemical purities in the range of 90–94% (Fig. 5). Furthermore, ^{64}Cu-DOTA-Annexin V is being evaluated in the same animal model of anti-Fas MoAb-induced hepatic apoptosis as described for ^{94m}Tc-Hynic-Annexin V.

When compared with ^{94m}Tc, the longer half-life of ^{64}Cu (physical half-life of ^{64}Cu=12.7 h, $E_{max}\beta^{+}$=0.578, 0.65 MeV) should provide a significantly wider time frame for in vivo monitoring of apoptosis in humans, whereas the lower β^{+} energy of the radionuclide should result in a decreased radiation burden to the patients' organs, in particular to the kidneys, spleen and liver. Hence, in spite of a slightly more complex synthesis, ^{64}Cu-DOTA-Annexin V may be suitable for application as a PET ligand in apoptosis imaging, especially in clinical settings.

$^{67/68}$Gallium-DOTA-Annexin V

Simultaneously with the development of ^{64}Cu-DOTA-Annexin V, the protein has also been radiolabelled with ^{67}Ga and ^{68}Ga using the same methodology (Fig. 5) [194]. Activation of the DOTA chelator with EDC and sulpho-NHS was nearly identical, resulting in a conjugation ratio of 3.7 molecules of DOTA/Annexin V. The final radiolabelling step with the gallium isotopes showed only minor differences in reaction conditions and reagents compared with the ^{64}Cu labelling. Immunoreactivity testing of the radioligands revealed comparable biological activity of ^{67}Ga-DOTA-Annexin V with ^{99m}Tc-Hynic-Annexin, which in turn was superior to ^{68}Ga-DOTA-Annexin V.

Dual-isotope biodistribution studies in mice and rats injected with a mixture of ^{67}Ga-DOTA-Annexin V and ^{99m}Tc-Hynic-Annexin V clearly revealed a rapid blood clearance over time for both tracers. However, the blood clearance was obviously better in the case of ^{99m}Tc-Hynic-Annexin V. In contrast, at 2 h p.i. the ^{99m}Tc radioactivity levels were significantly higher than the ^{67}Ga levels in the lungs, liver, spleen and gastro-intestinal tract, whereas kidney and heart uptake were similar. These preliminary biodistribution results seem to suggest that ^{67}Ga-DOTA-Annexin V could be useful as an alternative SPECT ligand for imaging apoptosis by providing higher signal-to-noise ratios. In addition, slower but more sustained tumour uptake might be achieved with ^{67}Ga-DOTA-Annexin V owing to its longer retention time in the blood compartment relative to ^{99m}Tc-Hynic-Annexin V.

Alternatively, first micro-PET studies in rats treated with anti-Fas MoAb to induce hepatic apoptosis showed increased liver uptake of ^{68}Ga-DOTA-Annexin V by a factor of 4.4 compared with control animals. Thus, the PET counterpart of ^{67}Ga-DOTA-Annexin V could offer new possibilities in PET imaging of apoptosis in spite of its lower in vitro biological activity. Nevertheless, the high-energy positron emission characteristics of ^{68}Ga (physical half-life of ^{68}Ga=1.135 h, $E_{max}\beta^{+}$=1.9 MeV) might hamper its application in the clinic by depositing a high radiation burden to specific organs such as the kidneys or liver. In contrast, ^{67}Ga-DOTA-Annexin V (physical half-life of ^{67}Ga=3.26 days, $E_{max}\gamma$=0.300, 0.393 MeV) exhibits a much longer half-life, allowing extensive in vivo monitoring of apoptotic processes over a wide time frame while emitting gamma rays at the upper detection limit of SPECT cameras.

^{18}F- and ^{99m}Tc-labelled radiopeptides

In the broad group of recently developed apoptosis-detecting radioligands, a radiopeptide construct was described, based on the AFIM molecule. Boisgard et al.

succeeded in engineering a small 8-kDa mini-protein derived from the specific PS-binding domain of the annexins which contains a multifunctional site for radiolabelling with either an ^{18}F tag, such as the ^{18}F-labelled maleimide reagent [195, 196], or ^{99m}Tc [197, 198]. Both radiolabelling methods yielded very high specific activities (i.e. 490–4,370 GBq/μmol) with excellent radiochemical purity of >99%. Furthermore, the AFIM construct was characterised by a high thermodynamic stability and high affinity for PS-containing membranes. Both tracers were also evaluated for tumour uptake in several melanoma mouse models of chemotherapy-induced apoptosis at various time points until 72 h following therapy administration [199]. ^{18}F-AFIM was excreted predominantly through the kidneys, with minor uptake in the liver and gastro-intestinal tract whereas ^{99m}Tc-AFIM was exclusively excreted by the kidneys without showing uptake in any of the other organs. In addition, extremely fast blood clearance was reported for the ^{99m}Tc-AFIM molecule, with removal from the blood compartment within 10 min p.i. Tracer uptake was reported in treated tumours only at 72 h post chemotherapy and in some untreated tumours, presumably reflecting spontaneous ongoing apoptosis.

The biological rationale for engineering a small 8-kDa mini-protein derived from the specific PS-binding domain of the annexins is very interesting because such peptide-like molecules could benefit from the favourable biodistribution characteristics that small peptides in general exhibit over bigger proteins. However, reducing the molecular structure of Annexin V by stripping of most of its 319 amino acids in order to retain a PS-binding core seems a very challenging undertaking for many reasons. In particular, such a drastic reduction in molecular size and integrity could result in major conformational changes, thereby affecting the stability and high affinity of the protein for binding PS residues. Most surprisingly, Boisgard et al. reported that the AFIM construct was characterised by a high thermodynamic stability and high affinity for PS-containing membranes. Unfortunately, no real evidence was provided to support these preliminary findings. Additionally, no concrete data have so far been presented on the molecular structure of the AFIM mini-protein that would allow true comparison with Annexin V or with the highly conserved consensus sequence found in all Annexins, which contains two of the most important PS-binding sites [175]. Although the concept of a multipurpose radiolabelling site, allowing both ^{18}F and ^{99m}Tc chemistry, is most interesting, the structural information on which this approach is based remains unclear. In spite of the very high specific activities obtained by this method, the in vitro and in vivo stability of the corresponding radioligands still needs to be fully demonstrated.

Both radiolabelled AFIM molecules, and ^{99m}Tc-AFIM in particular, seem to be cleared from the body more rapidly than ^{99m}Tc-Hynic-Annexin V owing to a very fast blood clearance followed by a predominant and rapid kidney clearance. However, whether the significantly increased blood clearance will contribute to higher tumour-to-background ratios when studying chemotherapy-induced apoptosis will greatly depend on the tumour's extraction efficiency and clearance. The fact that Boisgard et al. were unable to demonstrate ongoing tumour apoptosis within 24 and 48 h post therapy, in contrast to many other in vivo studies, might indicate that the radiolabelled AFIM ligands are cleared from the body too quickly to allow sufficient uptake and subsequent visualisation of apoptotic tumour cells. Furthermore, the lack of any semi-quantitative biodistribution data for ^{18}F-AFIM and ^{99m}Tc-AFIM in the described tumour models makes it impossible at present to compare organ and tumour uptake values with those reported for other apoptosis-detecting radioligands. Furthermore, the use of 2-deoxy-2-[^{18}F]fluoro-D-glucose (^{18}F-FDG) as a positive control tracer for ^{99m}Tc-AFIM tumour uptake does not seem to be a good choice for proving the specificity of the apoptotic signal. Although ^{18}F-FDG is being widely used to measure the glucose metabolism in a variety of organs and disease states, this tracer is unable to detect apoptotic or necrotic cell death by a specific mechanism of action.

Anti-PS monoclonal antibodies

Externalised PS residues as the primary target molecule for early detection of apoptotic cell death in vivo may also serve as antigen-binding sites for anti-PS antibodies. This type of antibody, in addition to anti-cardiolipin and lupus anticoagulant (LAC) antibodies, belongs to the family of anti-phospholipid antibodies which are known to inhibit the procoagulant and pro-inflammatory activities that externalised PS residues exert. The presence of anti-PS auto-antibodies circulating in the blood has been correlated with an increased risk of recurrent arterial and venous thrombo-embolism, recurrent foetal loss and thrombocytopenia. These symptoms are often related to the autoimmune disease SLE and many other conditions, which are generally referred to as the anti-phospholipid syndrome (APS). However, with the first PS-targeting MoAbs being described, such molecules, when radiolabelled, could be considered as alternative markers for apoptosis detection. The 3G4 mouse anti-PS MoAb (IgG_3) has shown equal affinity for PS residues and PI residues whereas the 9D2 rat MoAb (IgM) exhibits predominant affinity for PS residues ($K_d \approx 0.1$ n*M*), which in fact appears to be 10- to 70-fold higher than observed for Annexin V. Nevertheless, the slow blood clearance associated with such antibodies, in some applications, could represent a major drawback to their use in nuclear medicine, indicating the need for construction of small PS-targeting antibody fragments with enhanced pharmacokinetic properties.

Most interestingly, anionic phospholipids such as PS have also been proposed as specific markers for tumour vasculature and consequently as potential targets for cancer imaging and therapy. Externalisation of PS residues not only seems to take place during PCD or platelet activation, but also can occur on the cell surface of viable endothelial cells in response to a variety of cellular stress factors and pathological conditions. The most prominent factors include inflammatory cytokines (e.g. IL-1α or TNFα), hypoxia/reoxygenation, thrombin, acidic conditions, H_2O_2 or combinations of hypoxia/reoxygenation and IL-1α or TNFα. A recent study by Ran et al. demonstrated that PS becomes exposed on the vascular endothelial cells of different types of apoptotic solid tumours in mice and that such PS translocation is most likely caused by stress factors similar to those described for normal endothelial cells [200]. Although PS-positive tumour endothelium mostly was found to be non-apoptotic, PS-positive vessels appeared to be located particularly in and around regions of necrotic and apoptotic tumour cells, where hypoxia, acidity, thrombosed blood vessels, infiltrating host leucocytes and cytokine secretion are commonly present. Thus, the breakdown of PS asymmetry and subsequent exposure of PS residues to the cell surface of tumour blood vessels and malignant cells seems directly related to the necrotic and apoptotic status of the tumour microenvironment.

Taking these findings into account, PS-directed MoAbs such as the 3SB mouse antibody are being developed by Peregrine Pharmaceuticals Inc. (Tustin, CA, USA) as potential vascular targeting agents (VTAs). The 3SB IgM antibody shows major reactivity to PS but not to any other phospholipid, except for phosphatidic acid, which is only a minor component of the plasma membrane. According to Ran et al., PS residues are ubiquitously expressed on tumour endothelial cells (i.e. approximately 3×10^6 molecules per cell) and are located on the luminal surface of the tumour's blood vessel endothelium in all regions of the tumours, which makes them directly accessible for binding to VTAs administered in the blood [200]. In addition, PS residues are known to be abundantly present on endothelial cells of a variety of solid tumours while being absent from endothelium in nearly all the normal tissues. These characteristics make PS residues interesting targets for cancer imaging and therapy.

In spite of these interesting hallmarks, the potential use of anti-PS MoAbs and radioimmunoconjugates thereof in cancer imaging through vascular targeting is a difficult objective. In contrast to endothelial cells of murine or bovine origin, which were used as an in vitro model in the study of Ran et al., human vascular endothelial cells are likely to respond to similar cellular stress factors in a totally different way, possibly without causing any PS expression. Hence, extensive research is required to investigate the clinical applicability of using endothelial PS exposure as a target for vascular targeting and cancer imaging. Previous studies on tumour neoangiogenesis have demonstrated that the vascular structure of neoplastic tissues is often characterised by many "leaky" blood vessels, easily allowing passive diffusion of molecules into the tumour's microenvironment [201]. On the other hand, the extent of neovascularisation might differ from one tumour type to another. Taking these considerations into account, it remains to be seen whether specific tumour uptake by radiolabelled anti-PS MoAbs can actually be achieved by significantly increased PS expression on the tumour's vasculature, rather than by increased vascular permeability or vascularisation contributing to a specific tracer uptake. Other potential risks related to the clinical use of radiolabelled anti-PS MoAbs, such as the HAMA response, might be circumvented by generating chimerised or fully humanised variants.

Alternative radioligands

Anti-Annexin V monoclonal antibodies

Like the typical anti-phospholipid auto-antibody LAC, which is a well-known risk factor for thrombosis and recurrent spontaneous abortion, extracellular Annexin V can act as a pathogenic factor by providing an antigenic stimulus for auto-antibody formation. Thus, as for the anti-phospholipid auto-antibodies described earlier, significantly elevated concentrations of anti-Annexin V MoAbs have been found in sera from patients with rheumatoid arthritis, SLE, arterial or venous thrombosis, intrauterine fetal loss, pre-eclampsia and prolonged activated partial thromboplastin time. Furthermore, anti-Annexin V MoAbs present in sera from patients with SLE have been shown to exhibit anti-phospholipid and LAC properties [202–205].

As a result of these studies, several anti-Annexin V MoAbs were generated which could be radiolabelled for apoptosis imaging purposes. The majority of commercially available MoAbs are mouse (IgG_1 or $IgG_{2a/κ1}$), rabbit (IgG) and goat (IgG)-anti-human Annexin V specific MoAbs. At present, only one radiolabelled MoAb directed against human Annexin V has been described, by Kobayashi et al., who evaluated an ^{111}In-DTPA anti-Annexin V MoAb in a rat model of myocardial ischaemia–reperfusion injury (IR) [206, 207] as well as in rats with myocardial infarction (MI) [208]. These studies assumed that Annexin V exists in the soluble fraction of the healthy myocardium and is translocated to the myocardial cell membrane after transient acute ischaemia, thereby becoming accessible for binding to Annexin V-directed MoAbs. Twenty-four hour planar images of rats at 2, 7, 14 and 21 days post IR showed significantly increased tracer uptake in the heart compared with control animals. The difference in myocardial tracer accumulation was highest at 2 days after onset of ischaemia (i.e.

heart/lung ratio 3.32 vs 1.41 in controls) and gradually diminished over time until it became nearly insignificant at 50 days post IR. Macro-autoradiography revealed that ^{111}In-DTPA anti-Annexin V MoAb radioactivity was mainly located in the ischaemic area of the myocardium and in the left anterior descending coronary region of ischaemic rats owing to the left coronary artery occlusion used to induce transient myocardial ischaemia. In rats with acute MI, the increase in myocardial tracer uptake was even slightly higher compared with the corresponding IR rat group at 7 days after onset. The radioligand accumulated predominantly in the marginal area of the infarcted tissue as demonstrated by autoradiography. These preliminary data seem to suggest that radiolabelled anti-Annexin V MoAbs might be used for in vivo detection of myocardial ischaemia and cell death. Nevertheless, additional information is required to clearly demonstrate the specificity of antibody binding to Annexin V molecules as well as its clinical applicability. Furthermore, the mechanisms by which intracellular Annexin V becomes translocated to the outer side of the cell membrane and the pathological conditions associated with this phenomenon still need to be elucidated. In fact, more recent studies have revealed that the end-stage of heart failure in humans is characterised by a marked over-expression of Annexin II, V and VI along with a translocation of Annexin V from cardiomyocytes to interstitial cardiac tissue [209, 210].

A second approach in which radiolabelled anti-Annexin V MoAbs could be used as alternative radioligands for apoptosis imaging would consist in the pre-targeting concept that has been successfully applied in radioimmunodetection and radioimmunotherapy of tumour growth for several years. Considering the stoichiometry of Annexin V binding to externalised PS residues, some studies have demonstrated that, in theory, four to eight Annexin V molecules can bind to a single PS residue [100]. Hence, the apoptotic signal initially generated by PS exposure in early apoptotic cells could be amplified through binding with exogenously administered "cold" Annexin V, which in turn would act as a secondary target molecule. In a second step, the radiolabelled anti-Annexin V MoAb would then be injected in order to bind to the Annexin V moeities locally presented in the region of ongoing apoptosis. Evidently, such an approach would need to overcome the classical problems associated with antibody pre-targeting. In this case, endogenous Annexin V molecules circulating in the blood might interfere with the MoAb binding, thereby contributing to a high overall background radioactivity and to a higher radiation dose to specific organs. Although extracellular Annexin V under normal physiological conditions is present in very low concentrations in the blood compartment (i.e. 1–6 ng/ml), it should be considered as a possible interfering factor, especially in pathological conditions such as myocardial infarction which are characterised by a more than tenfold increase in the endogenous blood concentration of the protein [45, 211]. On the other hand, taking the fast bi-exponential blood clearance of human Annexin V into account, non-PS-bound Annexin V should be sufficiently cleared from the blood upon administration in order to provide a strong apoptotic signal for radioligand binding. Therefore, the use of radiolabelled antibodies directed against the Annexin V protein as target molecule might constitute an alternative approach in apoptosis imaging.

Radiolabelled caspase inhibitors and substrates

Amongst the group of newly developed radioligands directed against alternative target molecules involved in the apoptosis cascade, the use of radiolabelled caspase inhibitors probably represents one of the most innovative but also most tantalising approaches. Caspases are a family of cysteine-containing aspartate-specific proteases which play a key role in the apoptotic process. The caspases are synthesised intracellularly as inactive proenzymes essentially in all animal cells and are activated by cleavage at specific aspartate-cleaving sites in order to release a N-terminal pro-domain, leaving a large (∼20 kDa) and a small subunit (∼10 kDa) to heterodimerise. The active enzyme is a tetramer composed of two such heterodimers, which are primarily associated through interaction of the small subunits. The active protease can in turn sequentially activate other caspases, thereby generating a cascade which will eventually cause mitochondrial release of pro-apoptotic molecules [212–214]. Since caspase activation occurs in the early phase of the intracellular signalling process of cells undergoing apoptosis, radiolabelled caspase inhibitors could offer a valuable and highly specific tool for early detection of apoptosis. Furthermore, targeting of activated caspases is believed to be more specific in apoptosis detection than the PS-targeting approach, where necrotic cells can also contribute to the cell death signal. Many types of caspase inhibitors and caspase substrates have been constructed for the different members of the caspase family, each with different specificity. However, the group of fluoromethylketone (fmk) caspase inhibitors exhibit the most favourable characterisitics since they are highly cell permeable, soluble and irreversible in action while possessing an extended biological half-life and lower cytotoxicity in vivo compared with other groups. Amongst these, benzyloxycarbonyl-Val-Ala-DL-Asp (*O*-methyl)-fmk, designated Z-VAD-fmk, is one of the most commonly used caspase inhibitors with broad-spectrum activity.

In a study published by Haberkorn et al., ^{131}I-labelled Z-VAD-fmk was evaluated as an alternative in vivo marker for PCD through targeting and irreversible trapping by caspase inhibitors [215]. Successful radioiodination of the phenyl moiety of the *N*-terminal z-protection group clearly depended on the presence of carrier iodide,

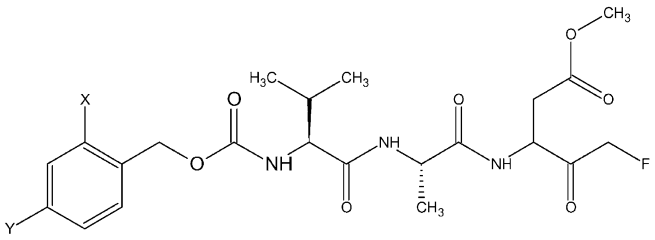

Fig. 6. Chemical structure of the 4-iodophenyl derivative (Y) and 2-iodophenyl derivative (X) of [^{131}I]IZ-VAD-fmk which were generated in radiochemical yields of >60 and <40, respectively. X and Y both represent ^{131}I

resulting in moderate radiochemical yields (i.e. 70%) and specific activities of about 3.3 GBq/μmol. However, the Tl(TFA)$_3$/[^{131}I]iodide labelling method generated a mixture of 2-iodophenyl and 4-iodophenyl derivatives which could not be separated on RP-HPLC (Fig. 6). Changing the order in which Z-VAD-fmk was reacted with Tl(TFA)$_3$ and [^{131}I]iodide did not affect the 4-iodophenyl product yield (i.e. 61%). Subsequently, in vitro [^{131}I]IZ-VAD-fmk uptake was investigated in Morris hepatoma (MH3924Atk8) cells expressing the herpes simplex virus thymidine kinase (*HSVtk*) gene, in which apoptosis was induced by ganciclovir treatment. Intracellular uptake of [^{131}I]IZ-VAD-fmk was increased merely twofold 24 h post treatment when compared with controls and remained nearly unchanged in both groups when the incubation time was increased up to 4 h. In contrast, 23% apoptotic cells were found in the TUNEL assay 24 h after ganciclovir therapy compared with 1.3% immediately after therapy administration, whereas "cold" IZ-VAD-fmk had shown a similar inhibition potency as Z-VAD-fmk towards apoptotic BJAB and SKW6 cells. In addition, the ^{131}I-labelled oligopeptide exhibited a rather poor absolute cellular uptake (i.e. 0.76% of the activity accumulated in untreated MH3924Atk8 cells), characterised by a slow transport mechanism of passive diffusion.

In view of all these radiochemical and biological problems associated with radiolabelled caspase inhibitors, many hurdles still need to be overcome before successful apoptosis imaging can be achieved. Furthermore, it is unclear whether the concentration of activated caspases generated in apoptotic cells will be high enough to provide sufficient radioligand accumulation for in vivo imaging. In this regard, radiolabelled caspase substrates might be more attractive candidates for metabolic trapping. Such an approach would entail delivery of radiochelated caspase substrates into the apoptotic cell, which would then be cleaved by activated caspases, leading to accumulation of radioactive hydrophilic metabolites. Since all activated caspases can repeatedly cleave multiple substrates during the apoptotic cascade in the cell, this approach could result in a significant amplification of the tracer signal, thereby enhancing the target-to-background ratio. In fact, more than 280 caspase substrates have been identified to date, providing an impressive amount of target molecules for caspase cleavage [216]. In addition, further progress is being made on the ^{18}F radiochemistry of fmk derivatives, which will provide new opportunities in the fluorination of fmk-based caspase inhibitors [217].

MMP-targeting radioligands

As previously mentioned, the mitochondria play a key role in the initiation of both apoptotic and necrotic cell death. The mitochondrial permeability transition pore (MPTP) is assumed to represent a high-conductance unselective channel between the inner and outer mitochondrial membranes whose opening is triggered by several physiological effectors, such as elevated matrix [Ca^{2+}], reduced concentrations of adenine nucleotides, reactive oxygen species or pH changes. The MPTP opening (i.e. often described as "mitochondrial permeability transition") causes a sudden increase in the permeability of the inner mitochondrial membrane to molecules smaller than 1.5 kDa, which results in uncoupling of the respiratory chain, immediate dissipation of the proton-dependent mitochondrial transmembrane potential ($\Delta\Psi_m$, MMP) and interruption in ATP synthesis followed by massive osmotic swelling of the mitochondria. Finally the outer mitochondrial membrane is disrupted with release of intermembrane components such as cytochrome *c*, procaspase-9, apoptosis-inducing factor and endonuclease G, which cause the cell to undergo apoptosis through caspase activation. In contrast, a high membrane potential, a low pH and cyclosporin A (CsA) provide protection against MPT [218–221]. During the apoptotic process, the MMP is being disrupted before caspase and endonuclease activation occur and this disruption even precedes PS exposure on the cell surface as well as morphological signs of apoptosis. The MMP collapse provoked at the high irreversible level of MPTP conductance is also considered as the point of no return in the apoptotic process and therefore represents an attractive and specific target for early detection of cells committed to die [9, 222–225].

Recently, Madar et al. developed a series of lipophilic MMP-dependent fluoro-phosphonium cations for PET imaging of apoptosis. For this purpose, several triphenyl methyl-phosphonium derivatives were radiolabelled with ^{18}F and evaluated for chemical and metabolic stability in vitro while their biodistribution was studied in rodents and mongrel dogs by PET imaging [226]. Among the group of fluorinated phosphonium analogues, [^{18}F]*p*-fluorobenzyltriphenyl-phosphonium cation, [^{18}F]*p*-FBnTP, showed the most favourable metabolic stability while exhibiting an extremely rapid blood clearance in mongrel dogs ($T_{1/2}$=12 s). Furthermore, the high, sustained tracer accumulation in multiple organs

could be reduced by 87% when MMP loss was induced. Biodistribution studies in mice and rats revealed a fast and predominant radioactivity uptake in the heart, followed by lungs, kidneys, muscle and liver. In addition, a 40–60% regional decrease in myocardial [^{18}F]*p*-FBnTP uptake could be documented in mongrel dogs with heart failure-induced cardiomyopathy. These findings were in accordance with the typical changes related to heart failure such as dilatation of the ventricles and thinning of the posterior heart wall [227]. These preliminary studies indicate that the heart represents the main target organ for [^{18}F]*p*-FBnTP uptake. Consequently, radiolabelled MPP markers such as [^{18}F]*p*-FBnTP show potential for in vivo detection of myocardial cell death by means of PET imaging.

In vitro models of taxotere-induced apoptosis in lung and prostate carcinoma cells also demonstrated a significant decrease in [^{18}F]*p*-FBnTP uptake of 54% and 43%, respectively. Furthermore, the decrease in tracer accumulation correlated inversely with the extent of taxotere-induced apoptosis as determined by TUNEL staining. Additionally, breast carcinoma-bearing nude mice treated with taxotere showed 45% lower tracer uptake in tumours at 48 h post therapy compared with control animals [228]. Similar results were achieved in a rat model of prostatic apoptosis, where lobe-specific decrease in [^{18}F]*p*-FBnTP accumulation (i.e. ranging from 45% to 58%) was observed between 2 and 4 days after androgen depletion [229]. Most interestingly, the differences in tracer uptake in the apoptotic prostate lobe were more pronounced than the changes in TUNEL-positive cells. Therefore, in vivo monitoring of the MMP collapse could represent a more sensitive method for early detection of apoptosis compared with existing methods such as the TUNEL assay directed against DNA laddering. Moreover, the MMP is considered to be a more accurate predictive parameter for cell death than caspase activation, which is often not required to generate apoptosis [220]. Taking these data into account, MMP-dependent biomarkers such as [^{18}F]*p*-FBnTP could represent a useful group of new radioligands for early evaluation of chemo- or radiotherapy-induced apoptosis. $\Delta\Psi_m$ disruption is a constant hallmark of apoptosis which has been found in a broad variety of cell types [222, 224]. Nevertheless, some cell types have been reported to undergo apoptosis without demonstrating early changes in $\Delta\Psi_m$ or inhibition of CsA [218]. Consequently, MMP-dependent radioligands might not be applicable for apoptosis detection in such cell types.

In addition to the MMP-targeting radioligands, the effect of apoptosis-inducing drugs which act on the $\Delta\Psi_m$ can also be monitored indirectly by using radiolabelled Annexin V. The flavanoid quercetin in particular has been shown to induce apoptosis by triggering a secondary $\Delta\Psi_m$ decrease which could be detected by a 50% increase in ^{99m}Tc-Annexin V uptake in both sensitive and drug-resistant cells [230].

Alternative imaging modalities

MRS/MRI

Apart from radionuclide imaging, magnetic resonance spectroscopy (MRS) is currently the only clinically available method for non-invasive in vivo detection and quantification of apoptosis. The changes in lipid structure and fluidity of the cell membrane which take place during the apoptotic process generate a number of small molecules (e.g. cytoplasmic lipid bodies, choline metabolites) which can be directly monitored by water-suppressed lipid ^{1}H MRS techniques. Several in vitro studies have reported on the appearance of mobile lipid signals in ^{1}H NMR spectra of cells induced to undergo apoptosis by treatment with chemotherapeutic drugs or anti-Fas MoAbs [231–234]. Furthermore, Blankenberg et al. demonstrated that lipid ^{1}H MRS allows direct quantification of the present fraction of apoptotic cells based on the increase in intensity of the hydrocarbon chains' methylene over methyl signals [235]. Nevertheless, a more recent in vivo study from Valonen et al. clearly indicated that apoptotic brain tumours derived from *HSV-tk*-transfected BT2C glioma cells did not show any increase in CH_2/CH_3 signal but rather a late occurring decrease [233]. Thus, these preliminary findings on MRS need to be addressed with some scepticism and require further investigation.

Apart from lipid ^{1}H MRS, apoptosis can also be detected indirectly by means of ^{31}P and ^{13}C MRS [236, 237]. In this case, the detection mode is based on the impaired high-energy phosphate metabolism typically associated with apoptotic cell death. Nevertheless, lipid proton spectroscopy offers several advantages over phosphorus MRS, which requires longer acquisition times while providing an inferior resolution. In general, MRS seems not to be very suitable for routine use in critically ill patients, and in vivo detection of apoptosis through MRS is significantly limited by relatively low sensitivity and poor temporal and spatial resolution [235, 238, 239]. In this regard, non-invasive radionuclide imaging of apoptosis should prove more useful than lipid proton nuclear MRS.

Since the morphological features associated with apoptosis (i.e. cell shrinkage and membrane blebbing) induce alterations in tissue water T2 and T1ρ relaxation times and apparent diffusion coefficient (ADC), magnetic resonance imaging (MRI) has also been investigated as an alternative technique for the in vivo detection of apoptosis [236, 240, 241]. In comparison with MRS techniques, ^{1}H MRI provides a much better spatial and temporal resolution along with a very high sensitivity. However, the changes in MR image contrast based on cell shrinkage and membrane blebbing are unable to provide an early indication of the ongoing apoptosis since these morphological features occur quite late in the apoptotic process. At present, the most successful ap-

proach in MRI for in vivo detection of apoptosis uses the highly specific and tight binding of Annexin V or synaptotagmin I to externalised PS residues. Since the C_2 domain of synaptotagmin I is known to bind to membrane-bound anionic phospholipids similar to Annexin V [242, 243], the protein was recently conjugated with superparamagnetic iron oxide nanoparticles (SPIO) and evaluated in vitro and in vivo in a murine EL4 lymphoma tumour model [244]. In a comparable way, cross-linked iron oxide nanoparticles (CLIO) were attached to Annexin V and tested in vitro [245]. In the case of the C_2-labelled SPIO particles, T2-weighted MRI images of tumour-bearing C57/B16 mice treated with cyclophosphamide/etoposide showed a significant and progressive decrease in tumour signal intensity compared with control animals. Tumour regions displaying the biggest MRI changes correlated well with areas containing the highest amount of apoptotic and necrotic cells. Similarly, T2-weighted imaging sequences of camptothecin-treated Jurkat T cells (i.e. 65% apoptotic cells) incubated with increasing concentrations of Annexin V-CLIO particles indicated a stronger, dose-dependent decrease in signal intensity versus untreated control cells (i.e. 12% apoptotic cells). Analogous control experiments with non-labelled CLIO did not show a significant decline in T2 relaxation times for apoptotic and control cells in any concentration. Thus both described contrast agents seem to offer considerable potential for successful detection of apoptosis by MRI. Furthermore, Gd-DTPA has been used successfully to assess the transmural extent of myocardial necrosis in patients with previous myocardial infarction by means of contrast-enhanced MRI [246].

Optical/bioluminescence imaging

In effort to develop a non-invasive optical imaging modality for in vivo detection of tumour apoptosis, Annexin V was recently conjugated with a near-infrared fluorochrome, cyanine-5.5 (Cy5.5) [247]. First in vivo data in irradiated MCA-29 tumour-bearing nude mice showed increased Cy5.5-Annexin V accumulation in tumours compared with untreated animals. Most interestingly, optical imaging allowed repeated acquisitions over a time course of 10 days owing to the high stability of the fluorochrome. Consequently, this approach could resolve many of the problems related to several apoptosis-detecting radioligands, including high cost, limited stability and a limited time window for consecutive apoptosis detection due to a short physical half-life. However, its biggest advantage is undoubtedly its capacity to monitor ongoing apoptosis in real time, which permits examination of the affected organs as the imaging procedure is proceeding, without requiring any additional signal processing. Such real-time examinations are particularly valuable when studying organs in motion, like the beating heart. Furthermore, real-time imaging of spontaneous or therapy-induced apoptosis could facilitate and speed up clinical decision-making in many pathological conditions. Therefore, near-infrared fluorescence imaging with Cy5.5-Annexin V seems to offer a promising new tool for in vivo detection of apoptotic cell death.

Another approach in bioluminescence imaging (BLI) that has emerged recently consists in using firefly luciferase, which is known as a useful reporter gene in vivo, allowing non-invasive detection of tumour growth or efficacy of drug treatment. Mandl et al. used this technique to investigate the spatial relationship over time between chemotherapy-induced tumour apoptosis and total tumour burden assessed by BLI [248]. Micro-SPECT images of Balb/c mice bearing luciferase-tranfected BCL-1 lymphomas indicated a significant increase in ^{99m}Tc-Hynic-Annexin V starting 3 h after doxorubicin treatment and peaking at 5 h post therapy. As shown by BLI, the tumour cell number started to decrease around 9 h post therapy. Thus, the luciferase reporter gene approach seems to offer new perspectives for monitoring apoptosis-related cell loss in tumour therapy.

Complementary to radionuclide imaging, biotin-labelled and fluorescent Annexin V has been applied with success for ex vivo detection and confirmation of ongoing apoptosis in different animal models of myocardial and cerebral ischaemia [155, 249, 250], atherosclerosis [251] and organ development [252]. Unfortunately, visible light (including fluorescent light) is by convention unable to penetrate more than 1–2 mm into biological tissue, which makes contrast agents like biotinylated or FITC-Annexin V unsuitable for in vivo detection applications. Even strongly fluorescent probes have been reported to visualise tumours only up to a maximum depth of 2.2 mm [253]. In contrast, near-infrared light probes are able to detect lesions as deep as 1.5 cm from the tissue surface [254] and therefore seem better candidates for in vivo apoptosis detection in superficial tumours (e.g. of the head and neck or breast region). Dumont et al. successfully applied the strong fluorescent probe Annexin V-Oregon Green to image cardiomyocyte apoptosis at the single-cell level in murine hearts [255]. Although this method is capable of detecting apoptotic cell death in real time, the imaging procedure required opening of the chest, making it unsuitable for routine clinical application.

Ultrasound imaging

An alternative detection method that would also allow real-time monitoring of apoptosis is high-frequency (40–50 MHz) ultrasound imaging. Ultrasonic detection of apoptosis is based on the subcellular nuclear changes (e.g. chromatin condensation and DNA fragmentation) which cells undergo during the apoptotic process. These nuclear changes provoke a significant increase in the ultrasound backscatter amplitude in ultrasonograms of

apoptotic cell samples, which results in much brighter images. First evidence that ultrasound imaging is able to differentiate living cells from apoptotic or dead cells was provided by Czarnota et al. using an vitro model of cisplatin-induced acute myeloid leukemia AML-3 cells [256]. Twenty-four hours of cisplatin treatment induced apoptosis in 95% of the AML-3 cells, which corresponded with a two- to fivefold increase in the ultrasound backscatter signal of apoptotic vs living cells. Furthermore, the increase in the ultrasound signal showed a linear correlation with the progression of nuclear condensation and fragmentation [257]. Nevertheless, it remains very questionable whether this imaging technique would provide a significant detection signal in tumours or other pathological conditions, which express a much lower degree of ongoing apoptosis. Similar experiments in a rat model of cerebral and epidermal apoptosis induced by photodynamic therapy gave similar results. However, in these experiments ultrasonic detection was performed ex vivo or at the skin surface of the animals [257]. Hence, considering the low focal detection range in tissue (i.e. 9 mm), high-frequency ultrasound imaging seems less appropriate for successful in vivo imaging of apoptosis.

Conclusion

As our knowledge of the molecular mechanisms involved in PCD is rapidly expanding, small pieces of this immense, complex puzzle are being revealed day by day. These discoveries will provide researchers with new insights into the phenomenon of apoptosis which will guide them in their quest to create novel markers and imaging techniques that will allow non-invasive detection of this process. When all the presented data are reviewed, several important conclusions can be drawn which should facilitate the design of new strategies in the development and evaluation of apoptosis-detecting radioligands.

There is a high demand for well-defined in vitro and in vivo cell death models that fully reflect the ongoing apoptosis present in a variety of human pathological conditions. In this regard, the localisation, extent and kinetics of the PCD process over time need to be determined and compared very carefully. Hence, meticulous translation of animal data to human models remains very important in the design of clinical trials focussed on apoptosis imaging. Secondly, extensive characterisation of the optimal time frame for imaging chemo- and radiotherapy-induced apoptosis and determination of the optimal radioligand biodistribution time are still required. Complementary techniques such as flow cytometry, immunohistological staining methods and the TUNEL assay remain critical to assess the amount of ongoing apoptosis accurately in order to confirm the specificity of the apoptotic signal provided by the isotopic detection methods. In this regard, highly specific apoptosis-detecting radioligands that are able to discriminate apoptosis from other types of cell death would prove most valuable.

Continued efforts in the identification of novel molecular targets involved in the apoptotic cascade could contribute to new strategies that would allow early detection of the process by means of specific cell death radioligands. Furthermore, new imaging modalities are being explored in addition to the currently used radionuclide techniques, which will enable physicians to monitor in vivo apoptosis in real time. Evidently, such techniques will greatly improve clinical decision-making in apoptosis-related diseases. Furthermore, the therapeutic (i.e. apoptosis inhibition) or toxic (i.e. apoptosis induction) effect of new drugs can be evaluated by means of specific apoptosis tracers. Such markers could also allow physicians to monitor the efficacy of anti-cancer treatment and to select responding from non-responding patients at an early stage of chemo- or radiotherapy.

Finally, novel drug delivery approaches that would allow or facilitate sufficient administration of apoptosis markers like radiolabelled Annexin V into the brain could lead to successful cell death detection and quantification in many neurological disorders. Consequently, this methodology could open new frontiers in the diagnostic imaging of stroke, Parkinson's disease and Alzheimer's disease and further elucidate the role of neurological cell death in these pathologies.

References

1. Kerr JFR, Wyllie AH, Currie AR. Apoptosis: a basic biological phenomenon with wide-ranging implications in tissue kinetics. Br J Cancer 1972;26:239–57
2. Proskuryakov SY, Konoplyannikov AG, Gabai VL. Necrosis: a specific form of programmed cell death? Exp Cell Res 2003;283:1–16
3. McConkey DJ. Biochemical determinants of apoptosis and necrosis. Toxicol Lett 1998;99:157–68
4. Majno G, Joris I. Apoptosis, oncosis and necrosis: an overview of cell death. Am J Pathol 1995;146:3–15
5. Honig LS, Rosenberg RN. Apoptosis and neurologic disease. Am J Med 2000;108:317–30
6. Allen RT, Hunter WJ, Agrawal DK. Morphological and biochemical characterization and analysis of apoptosis. J Pharmacol Toxicol Methods 1997;37:215–28
7. Saraste A, Pulkki K. Morphologic and biochemical hallmarks of apoptosis. Cardiovasc Res 2000;45:528–37
8. Wyllie AH, Kerr JFR, Currie AR. Cell death: the significance of apoptosis. In: Bourne GH, Danielli JF, Jeon KW, eds. International review of cytology. London: Academic; 1980. pp. 251–306
9. Syeed SA, Vohra H, Gupta A, Ganguly NK. Apoptosis: molecular machinery. Curr Sci 2001;80:349–60
10. Böhm I, Schild H. Apoptosis: the complex scenario for a silent cell death. Mol Imaging Biol 2003;5:2–14
11. Bortner CD, Cidlowski A. A necessary role for cell shrinkage in apoptosis. Biochem Pharmacol 1998;56:1549–59

12. Denecker G, Vercammen D, Declercq W, Vandenabeele P. Apoptotic and necrotic cell death induced by death domain receptors. Cell Mol Life Sci 2001;58:356–70
13. Bridgham JT, Wilder JA, Hollocher H, Johnson AL. All in the family: evolutionary and functional relationships among death receptors. Cell Death Differ 2003;10:19–25
14. French LE, Tschopp J. Protein-based therapeutic approaches targeting death receptors. Cell Death Differ 2003;10:117–23
15. Schmitz I, Kirchhoff S, Krammer PH. Regulation of death receptor-mediated apoptosis pathways. Int J Biochem Cell Biol 2000;32:1132–6
16. Kaufmann SH. Activation of cell death pathways. Hematology 1999;476–82
17. Hengartner MO. The biochemistry of apoptosis. Nature 2000;407:770–7
18. Schimmer AD, Hedley DW, Penn LZ, Minden MD. Receptor- and mitochondrial-mediated apoptosis in acute leukemia: a translational view. Blood 2001;98:3541–53
19. Thompson CB. Apoptosis in the pathogenesis and treatment of disease. Science 1995;267:1456–62
20. Saikumar P, Dong Z, Mikhailov V, et al. Apoptosis: definition, mechanisms, and relevance to disease. Am J Med 1999; 107:489–506
21. Yue T-L, Ohlstein EH, Ruffolo Jr RR. Apoptosis: a potential target for discovering novel therapies for cardiovascular diseases. Curr Opin Chem Biol 1999;3:474–80
22. Bosman FT, Visser BC, Van Oeveren J. Apoptosis: pathophysiology of programmed cell death. Pathol Res Pract 1996;192:676–83
23. Kam PCA, Ferch NI. Apoptosis: mechanisms and clinical implications. Anaesthesia 2000;55:1081–93
24. Lowe SW, Lin AW. Apoptosis in cancer. Carcinogenesis 2000;21:485–95
25. Kerr JFR, Winterford CM, Harmon BV. Apoptosis: its significance in cancer and cancer therapy. Cancer 1994;73:2013–26
26. Zörnig M, Hueber AO, Baum W, Evan G. Apoptosis regulators and their role in tumorigenesis. Biochim Biophys Acta 2001;1551:1–37
27. Evan GI, Vousden KH. Proliferation, cell cycle and apoptosis in cancer. Nature 2001;411:342–8
28. White E. Life, death and the pursuit of apoptosis. Gene Dev 1996;10:1–15
29. Ashkenazi A, Dixit VM. Death receptors: signalling and modulation. Science 1998;281:1305–8
30. Evan G, Littlewood T. Apoptosis: a matter of life and cell death. Science 1998;281:1317–21
31. Green DR, Reed JC. Mitochondria and apoptosis. Science 1998;281:1309–12
32. Thornberry NA, Lazebnik Y. Caspases: enemies within. Science 1998;281:1312–6
33. Dive C, Hickman JA. Drug-target interactions: only the first step in the commitment to a programmed cell death? Br J Cancer 1991;64:192–6
34. Green AM, Steinmetz ND. Monitoring apoptosis in real time. Cancer J 2002;8:82–92
35. Belhocine T, Steinmetz N, Hustinx R, et al. Increased uptake of the apoptosis-imaging agent ^{99m}Tc recombinant human annexin V in human tumors after one course of chemotherapy as a predictor of tumor response and patient prognosis. Clin Cancer Res 2002;8:2766–74
36. Blankenberg FG, Narula J, Strauss HW. In vivo detection of apoptotic cell death: a necessary measurement for evaluating therapy for myocarditis, ischemia and heart failure. J Nucl Cardiol 1999;6:531–9
37. Gerke V, Moss SE. Annexins: from structure to function. Physiol Rev 2002;82:331–71
38. Benz J, Hofmann A. Annexins: from structure to function. Biol Chem 1997;378:177–83
39. Delmer DP, Potikha TS. Structures and functions of annexins in plants. Cell Mol Life Sci 1997;53:546–53
40. Tzima E, Walker JH. Platelet annexin V: the ins and outs. Platelets 2000;11:245–51
41. Swairjo MA, Seaton BA. Annexin structure and membrane interactions: a molecular perspective. Annu Rev Biophys Struct 1994;23:193–213
42. Van Heerde WL, de Groot PG. Reutelingsperger CPM. The complexity of the phospholipid binding protein annexin V. Thromb Haemost 1995;73:172–9
43. Weinman S. Calcium-binding proteins: an overview. J Biol Buccale 1991;19:90–8
44. Andree HAM, Reutelingsperger CPM, Hauptmann R, Hemker HC, Hermens WT, Willems GM. Binding of vascular anticoagulant α (VACα) to planar phospholipid bilayers. J Biol Chem 1990;265:4923–8
45. Römisch J, Schüler E, Bastian B, et al. Annexins I to VI: quantitative determination in different human cell types and in plasma after myocardial infarction. Blood Coagul Fibrinolysis 1992;3:11–7
46. Andree HAM, Stuart MCA, Hermens WT, Reutelingsperger CPM, Hemker HC, Frederik PM, Willems GM. Clustering of lipid-bound annexin V may explain its anticoagulant effect. J Biol Chem 1992;267:17907–12
47. Kirsch T, Harrison G, Golub EE, Nah H-D. The roles of annexins and types II and X collagen in matrix vesicle-mediated mineralization of growth plate cartilage. J Biol Chem 2000;275:35577–83
48. Matteo RG, Moravec CS. Immunolocalization of annexins IV, V and VI in the failing and non-failing human heart. Cardiovasc Res 2000;45:961–70
49. Walker JH, Boustead CM, Brown R, Koster JJ, Middleton CA. Tissue and subcellular distribution of endonexin, a calcium-dependent phospholipid-binding protein. Biochem Soc Trans 1990;18:1235–6
50. Walker JH, Boustead CM, Koster JJ, Bewley M, Walker DA. Annexin V, a calcium-dependent phospholipid binding protein. Biochem Soc Trans 1992;20:828–33
51. Murphy CT, Peers SH, Forder RA, Flower RJ, Carey F, Westwick J. Evidence for the presence and location of annexins in human platelets. Biochem Biophys Res Commun 1992;189:1739–46
52. Huber R, Römisch J, Paques EP. The crystal and molecular structure of human annexin V, an anticoagulant protein that binds to calcium and membranes. EMBO J 1990;9:3867–74
53. Huber R, Berendes R, Burger A, et al. Crystal and molecular structure of human annexin V after refinement. Implications for structure, membrane binding and ion channel formation of the annexin family of proteins. J Mol Biol 1992;223:683–704
54. Gerke V, Moss SE. Annexins and membrane dynamics. Biochim Biophys Acta 1997;1357:129–54
55. Andree HAM, Reutelingsperger CPM, Hauptmann R, Hemker HC, Hermens WT, Willems GM. Binding of vascular anticoagulant (VAC) to planar phospholipid bilayers. J Biol Chem 1990;265:4923–8
56. Ahn NG, Teller DC, Bienkowski MJ, McMullen BA, Lipkin EW, de Haën C. Sedimentation equilibrium analysis of five lipocortin-related phospholipase A_2 inhibitors from human placenta. J Biol Chem 1988;263:18657–63

57. Römisch J, Grote M, Weithmann KU, Heimburger N, Amann E. Annexin proteins PP4 and PP4-X: comparative characterization of biological activities of placental and recombinant proteins. Biochem J 1990;272:223–9
58. Tait JF, Gibson D, Fujikawa K. Phospholipid binding properties of human placental anticoagulant protein-I, a member of the lipocortin family. J Biol Chem 1989;264:7944–9
59. Vermes I, Haanen C, Steffens-Nakken H, Reutelingsperger C. A novel assay for apoptosis: flow cytometric detection of phosphatidylserine expression on early apoptotic cells using a fluorescein labelled annexin V. J Immunol Methods 1995;184:39–51
60. Tait JF, Smith C, Wood BL. Measurement of phosphatidylserine exposure in leukocytes and platelets by whole-blood flow cytometry with annexin V. Blood Cells Mol Dis 1999; 25:271–8
61. Zhang G, Gurtu V, Kain SR, Yan G. Early detection of apoptosis using a fluorescent conjugate of annexin V. Biotechniques 1997;23:525-31
62. Ormerod MG, Sun X-M, Brown D, Snowden RT, Cohen GM. Quntification of apoptosis and necrosis by flow cytometry. Acta Oncol 1993;32:417–24
63. Van Heerde WL, Robert-Offerman S, Dumont E, Hofstra L, Doevendans PA, Smits JFM, Daemen MJAP, Reutelingsperger CPM. Markers of apoptosis in cardiovascular tissues: focus on annexin V. Cardiovasc Res 2000;45:549–59
64. Sgonc R, Gruber J. Apoptosis detection: an overview. Exp Gerontol 1998;33:525–33
65. Kang PM, Izumo S. Apoptosis in heart failure: is there light at the end of the tunnel (TUNEL)? J Card Fail 2000;6:43–6
66. Darzynkiewicz Z, Bedner E, Traganos F. Difficulties and pitfalls in analysis of apoptosis. Methods in cell biology. London: Academic; 2001:527–46
67. Blankenberg FG, Tait JF, Strauss HW. Apoptotic cell death: its implications for imaging in the next millennium. Eur J Nucl Med 2000;27:359–67
68. Blankenberg FG, Ohtsuki K, Strauss HW. Dying a thousand deaths: radionuclide imaging of apoptosis. Q J Nucl Med 1999;43:170–6
69. Hofstra L, Liem IH, Dumont EA, et al. Visualisation of cell death in vivo in patients with acute myocardial infarction. Lancet 2000;356:209–12
70. Hofstra L, Dumont EA, Thimister PWL, et al. In vivo detection of apoptosis in an intracardiac tumor. J Am Med Assoc 2001;285:1841–2
71. Rao LVM, Tait JF, Hoang AD. Binding of annexin V to human ovarian carcinoma cell line (OC-2008). Contrasting effects on cell surface factor VIIa/tissue factor activity and prothrombinase activity. Thromb Res 1992;67:517–31
72. Funakoshi T, Heimark RL, Hendrickson LE, McMullen BA, Fujikawa K. Human placental anticoagulant protein: isolation and characterisation. Biochemistry 1987;26:5572–8
73. Tait JF, Sakata M, McMullen BA, Miao CH, Funakoshi T, Hendrickson LE, Fujikawa K. Placental anticoagulant proteins: isolation and comparative characterisation of four members of the lipocortin family. Biochemistry 1998;27:6268–76
74. Wood BL, Gibson DF, Tait JF. Increased erythrocyte phosphatidylserine exposure in sickle cell disease: flow-cytometric measurement and clinical associations. Blood 1996;88:1873–80
75. Tait JF, Engelhardt S, Smith C, Fujikawa K. Prourokinase-Annexin V chimeras. J Biol Chem 1995;270:21594–9
76. Thiagarajan P, Benedict CR. Inhibition of arterial thrombosis by recombinant annexin V in a rabbit carotid artery injury model. Circulation 1997;96:2339–47
77. Reutelingsperger CPM, van Heerde WL. Annexin V, the regulator of phosphatidylserine-catalyzed inflammation and coagulation during apoptosis. Cell Mol Life Sci 1997;53:527–32
78. Williamson P, Schiegel RA. Back and forth: the regulation and function of transbilayer phospholipid movement in eukarotic cells. Mol Membr Biol 1994;11:199–216
79. Schroit AJ, Zwaal RFA. Transbilayer movement of phospholipids in red cell and platelet membranes. Biochim Biophys Acta 1991;1071:313–29
80. Zwaal RFA, Schroit AJ. Pathophysiologic implications of membrane phospholipid asymmetry in blood cells. Blood 1997;89:1121–32
81. Bevers EM, Comfurius P, Dekkers DWC, Zwaal RFA. Lipid translocation across the plasma membrane of mammalian cells. Biochim Biophys Acta 1999;1439:317–30
82. Martin Brown J, Wouters BJ. Apoptosis and cancer chemotherapy. Totowa: Humana; 1999:1–333
83. Hickman JA. Apoptosis induced by anticancer drugs. Cancer Metastasis Rev 1992;11:121–39
84. Hickman JA. Apoptosis and chemotherapy resistance. Eur J Cancer 1996;32A:921–6
85. Cohen-Jonathan E, Bernhard EJ, McKenna WG. How does radiation kill cells? Curr Opin Chem Biol 1999;3:77–83
86. Kessel D, Luo Y. Photodynamic therapy: a mitochondrial inducer of apoptosis. Cell Death Differ 1999;6:28–35
87. Dewey WC, Ling CC, Meyn RE. Radiation-induced apotosis: relevance to radiotherapy. Int J Radiat Oncol Biol Phys 1995;33:781–96
88. Susin SA, Zamzami N, Kroemer G. Mitochondria as regulators of apoptosis: doubt no more. Biochim Biophys Acta 1998;1366:151–65
89. Martin SJ, Reutelingsperger CPM, McGahon AJ, et al. Early redistribution of plasma membrane phosphatidylserine is a general feature of apoptosis regardless of the initiating stimulus: inhibition by overexpression of Bcl-2 and Abl. J Exp Med 1995;182:1545–56
90. Van den Eijnde SM, Boshart L, Reutelingsperger CPM, De Zeeuw CI, Vermeij-Keers C. Phosphatidylserine plasma membrane asymetry in vivo: a pancellular phenomenon which alters during apoptosis. Cell Death Differ 1997;4:311–6
91. Denecker G, Dooms H, Van Loo G, et al. Phosphatidyl serine exposure during apoptosis precedes release of cytohrome c and decrease in mitochondrial transmembrane potential. FEBS Lett 2000;465:47–52
92. Fadok VA, Savill JS, Haslett C, et al. Different populations of macrophages use either the vibronectin receptor or the phosphatidylserine receptor to recognize and remove apoptotic cells. J Immunol 1992;149:4029–35
93. Fadok VA, Voelker DR, Campbell PA, Cohen JJ, Bratton DL, Henson PM. Exposure of phosphatidylserine on the surface of apoptotic lymphocytes triggers specific recognition and removal by macrophages. J Immunol 1992;148:2207–16
94. Li MO, Sarkisian MR, Mehal WZ, Rakic P, Flavell RA. Phosphatidylserine receptor is required for clearance of apoptotic cells. Science 2003;302:1560–3
95. Sun J, Bird P, Salem HH. Interaction of annexin V and platelets: effects on platelet function and protein S binding. Thromb Res 1993;69:289–96
96. Thiagarajan P, Tait JF. Binding of annexin V/placental anticoagulant protein I to platelets. J Biol Chem 1990;265:17420–3

97. Tait JF, Gibson D. Measurement of membrane phospholipid asymmetry in normal and sickle-cell erythrocytes by means of annexin V binding. J Lab Clin Med 1994;123:741–8
98. Van Heerde WL, Poort S, Van't Veer C, Reutelingsperger CPM, De Groot PG. Binding of recombinant annexin V to endothelial cells: effect of Annexin V binding on endothelial-cell-mediated thrombin formation. Biochem J 1994; 302:305–12
99. Sugimura M, Donato R, Kakkar VV, Scully MF. Annexin V as a probe of the contribution of anionic phospholipids to the procoagulant activity of tumour cell surfaces. Blood Coagul Fibrinolysis 1994;5:365–73
100. Meers P, Mealy T. Calcium-dependent annexin V binding to phospholipids: stoichiometry, specificity, and the role of negative charge. Biochemistry 1993;32:11711–21
101. Stratton JR, Dewhurst TA, Kasina S, Reno JM, Cerqueira MD, Baskin DG, Tait JF. Selective uptake of radiolabeled annexin V on acute porcine left atrial thrombi. Circulation 1995;92:3113–21
102. Bevers EM, Comfurius P, Zwaal RFA. Changes in membrane phospholipid distribution during platelet activation. Biochim Biophys Acta 1983;736:57–66
103. Stuart MCA, Bevers EM, Comfurius P, Zwaal RFA, Reutelingsperger CPM, Frederik PM. Ultrastructural detection of surface exposed phosphatidylserine on activated blood platelets. Thromb Haemost 1995;74:1145–51
104. Fraker P, Speck J. Protein and cell membrane iodinations with a sparingly soluble chloroamide, 1, 3, 4, 6-tetrachloro-3a, 6a-diphenylglycoluril. Biochem Biophys Res Commun 1978;80:849–57
105. Tait JF, Gibson D. Measurement of membrane phospholipid asymmetry in normal and sickle-cell erythrocytes by means of annexin V binding. J Lab Clin Med 1994;123:741–8
106. Tait JF, Cerqueira MD, Dewhurst TA, Fujikawa K, Ritchie JL, Stratton JR. Evaluation of annexin V as a platelet-directed thrombus targeting agent. Thromb Res 1994;75:491–501
107. Goodwin CA, Wheeler-Jones C, Namiranian S, Bokkala S, Kakkar V, Authi KS, Scully MF. Increased expression of procoagulant activity on the surface of human platelets exposed to heavy-metal compounds. Biochem J 1991; 308:15–21
108. Kinlough-Rathbone RL, Perry DW. Prolonged expression of procoagulant activity of human platelets degranulated by thrombin. Thromb Haemost 1995;74:958–61
109. Le DT, Rapaport SI, Rao LVM. Studies of the mechanism for enhanced cell surface factor VII/tissue factor activation of factor X on fibroblast monolayers after their exposure to *N*-ethylmaleimide. Thromb Haemost 1994;72:848–55
110. Rao LVM, Tait JF, Hoang AD. Binding of annexin V to human ovarian carcinoma cell line (OC-2008). Contrasting effects on cell surface factor VIIa/tissue factor activity and prothrombinase activity. Thromb Res 1992;67:517–31
111. Tait JF, Engelhardt S, Smith C, Fujikawa K. Prourokinase-Annexin V chimeras: construction, expression, and characterization of recombinant proteins. J Biol Chem 1995; 270:21594–9
112. Lahorte C, Dumont F, Slegers G, Van De Wiele C, Dierckx RA, Philippé J. Synthesis and in vitro stability of ^{123}I-labelled annexin V: a potential agent for SPECT imaging of apoptotic cells. J Labelled Cpd Radiopharm 2000;43:739–51
113. Lahorte C, Slegers G, Philippé J, Van De Wiele C, Dierckx RA. Synthesis and in vitro evaluation of ^{123}I-labelled human recombinant annexin V. Biomol Eng 2001;17:51–3
114. Lahorte C, Van de Wiele C, Bacher K, et al. Biodistribution and dosimetry study of ^{123}I-rh-Annexin V in mice and humans. Nucl Med Commun 2003;24:871–80
115. Lahorte C, Pétillot P, Nevière R, Marchetti P, Slegers G. The myocardial uptake of ^{123}I-annexin V is increased in septic rats [abstract]. J Labelled Cpd Radiopharm 2001;44(Suppl 1):S430–2
116. Pétillot P, Lahorte C, Nevière R, Slegers G, Vallet B, Formstecher P, Marchetti P. Myocardial protection is provided by the caspase inhibitor zVAD.fmk during septic shock [abstract]. Intensive Care Med 2001;27(43 Suppl 2):S146
117. Lahorte C, Pétillot P, Marchetti P, Bonanno E, Signore A, Slegers G. Ex vivo detection of myocardial cell death with ^{123}I-annexin V in a rat model of septic shock [abstract]. Eur J Nucl 2002;29(Suppl 1):S91
118. World Health Organisation Technical Report Series 611. Use of ionizing radiation and radionuclides on human beings from medical research, training, and non-medical purposes. Report of a WHO Expert Committee, Geneva; 1977
119. Annals of the ICRP. Radiological protection in biomedical research. New York: Pergamon; 1991:12–3
120. Russell J, O' Donoghue JA, Finn R, et al. Iodination of Annexin V for imaging apoptosis. J Nucl Med 2002; 43:671–7
121. Glaser M, Collingridge DR, Aboagye E, et al. Preparation of [^{124}I]IBA-annexin-V as a potential PET probe for apoptosis [abstract]. J Labelled Cpd Radiopharm 2001;44(Suppl 1): S336–8
122. Glaser M, Collingridge DR, Aboagye EO, et al. Iodine-124 labelled annexin-V as a potential radiotracer to study apoptosis using positron emission tomography. Appl Radiat Isot 2003;58:55–62
123. Keen H, Dekker B, Disley L, Hastings D, Lyons S, Smith N, Zweit J, Watson A. Iodine-124 labelled annexin V for PET imaging of in vivo cell death [abstract]. J Nucl Med 2003;44(5):180
124. Dekker B, Keen H, Zweit J, Lyons S, Smith N, Watson A, Williams G, Disley L. Detection of cell death using ^{124}I-Annexin V [abstract]. J Nucl Med 2002;43(5):71P
125. Dekker B, Disley L, Hastings D, Keen H, Lyons S, Shaw D, Watson A, Zweit J. Use of [^{124}I]-4-iodobenzylsuccinimide to radiolabel MBP-Annexin V [abstract]. J Labelled Cpd Radiopharm 2003;46(Suppl 1):S386
126. Wester HJ, Hammacher K, Stöcklin G. A comparative study of n.c.a. fluorine-18 labeling of proteins via acylation and photochemical conjugation. Nucl Med Biol 1996;23:365–72
127. Wester HJ. Zur praktisch trägerfreien ^{18}F-fluorierung von Proteinen, Peptiden und Tyrosin. Berichte des Forschungszentrums Jülich [dissertation]. Germany: University of Cologne; 1996:3206
128. Zijlstra S, Gunawan J, Burchert W. Synthesis and evaluation of a ^{18}F-labelled recombinant annexin-V derivative, for identification and quantification of apoptotic cells with PET. Appl Radiat Isot 2003;58:201–7
129. Zijlstra S, Gunawan J, Burchert W. Synthesis of fluorine-18 labeled recombinant annexin V derivative, for identification and quantification of apoptotic cells with PET [abstract]. Abstracts of the IXth Turku PET symposium, May 25–28, 2002, Turku, Finland; 2002
130. Mease RC, Weinberg IN, Toretsky JA, Tait JF. Preparation of F-18 labeled annexin V: a potential PET radiopharmaceutical for imaging cell death [abstract]. J Nucl Med 2003; 44(5):295P–6P

131. Grierson JR, Yagle KJ, Eary JF, et al. Production of [F-18]fluoroannexin for imaging apoptosis with PET. Bioconjug Chem 2004; 15:373–9
132. Murakami Y, Takamatsu H, Tatsumi M, Noda A, Ichise R, Nishimura S. F-18 labeled annexin V: a PET tracer for apoptosis imaging [abstract]. J Nucl Med 2003;44(5): 312P
133. Kasina S, Rao TN, Srinivasan A, et al. Development and biologic evaluation of a kit for preformed chelate technetium-99m radiolabeling of an antibody Fab fragment using a diamide dimercaptide chelating agent. J Nucl Med 1991;32:1445–51
134. Fritzberg AR, Abrams PG, Beaumier PL, et al. Specific and stable labeling of antibodies with technetium-99m with a diamide dithiolate chelating agent. Proc Natl Acad Sci USA 1988;85:4025–9
135. Kown MH, Strauss HW, Blankenberg FG, et al. In vivo imaging of acute cardiac allograft rejection in human patients using ^{99m}technetium labeled annexin V. Am J Transplant 2001;1:270–7
136. Narula J, Acio ER, Narula N, et al. Annexin-V imaging for noninvasive detection of cardiac allograft rejection. Nat Med 2001;7:1347–51
137. Kemerink GJ, Boersma HH, Thimister PWL, et al. Biodistribution and dosimetry of ^{99m}Tc-BTAP-annexin-V in humans. Eur J Nucl Med 2001;28:1373–8
138. Van den Heuvel IJ, Pool B, Valdés-Olmos R, Haas R. Labelling and imaging aspects of ^{99m}Tc-rh-Annexin V in tumour-apoptosis detection [abstract]. Eur J Nucl Med Mol Imaging 2003;30(Suppl 2):S167
139. Haas RLM, Valdés-Olmos RA, De Jong D, Zerp SF, Van den Heuvel IJ, Hoefnagel CA, Bartelink H, Verheij M. Radiation induced apoptosis in follicular lymphoma patients assessed by ^{99m}Tc-Annexin V scintigraphy [abstract]. Eur J Nucl Med Mol Imaging 2003;30(Suppl 2): S197
140. Abrams MJ, Juweid M, tenKate CI, et al. Technetium-99m-human polyclonal IgG radiolabeled via the hydrazino nicotinamide derivative for imaging focal sites of infection in rats. J Nucl Med 1990;31:2022–8
141. Blankenberg FG, Katsikis PD, Tait JF, et al. In vivo detection and imaging of phosphatidylserine expression during programmed cell death. Proc Natl Acad Sci USA 1998; 95:6349–54
142. Blankenberg FG, Tait J, Ohtsuki K, Strauss HW. Apoptosis: the importance of nuclear medicine. Nucl Med Commun 2000;21:241–50
143. Narula J, Petrov A, Kolodgie FD, Acio ER, Snyder G, Tait JF, Blankenberg FG, Strauss HW. Transient sarcolemmal phosphatidyl serine expression as a marker of brief ischemia: an evaluation by ^{99m}Tc-Annexin V imaging [abstract]. J Nucl Med 2000;41(5):173P–4P
144. Kown MH, Van der Steenhoven T, Blankenberg FG, et al. Zinc-mediated reduction of apoptosis in cardiac allografts. Circulation 2000;102:III-228–32
145. Kown MH, Van der Steenhoven TJ, Jahncke CL, et al. Zinc chloride-mediated reduction of apoptosis as an adjunct immunosuppressive modality in cardiac transplantation. J Heart Lung Transplant 2002;21:360–5
146. Kemerink GJ, Liu X, Kieffer D, et al. Safety, biodistribution, and dosimetry of ^{99m}Tc-HYNIC-Annexin V, a novel human recombinant annexin V for human application. J Nucl Med 2003;44:947–52
147. Steinmetz N, Taillefer R, Hendel RC, et al. Simultaneous dual isotope ^{201}TI/^{99m}Tc-Annexin (apomate$^{TM)}$ SPECT in detection of acute myocardial infarction: initial results of a phase II multicenter trial [abstract]. J Nucl Med 2002;43(5):4P
148. Taillefer R, Phaneuf DC, Duong DH, et al. ^{99m}Tc-Annexin V scintigraphy in detection of acute myocardial infarction (MI): repeat imaging after the onset of acute symptoms in order to evaluate the persistence of abnormal radiotracer uptake [abstract]. J Nucl Med 2002;43(5):5P
149. Thimister PWL, Pakbiers M, Janssen D, Heidendal GAK. Disappearance of apoptosis in the sub acute phase of acute myocardial infarction [abstract]. Eur J Nucl Med Mol Imaging 2002;29(Suppl 1):S49
150. Kietselaer BL, Boersma HH, Heidendal GA, et al. The use of ^{99m}Tc labeled annexin-A5 imaging in the diagnostic work-up of intracardiac masses [abstract]. J Nucl Med 2003;44(5):156P
151. Van de Wiele C, Lahorte C, Vermeersch H, et al. Quantitative tumour apoptosis imaging using ^{99m}Tc-HYNIC-Annexin single photon emission computerized tomography. J Clin Oncol 2003;21:3483–7
152. Vermeersch H, Loose D, Lahorte C, et al. ^{99m}Tc-HYNIC Annexin-V imaging of primary head and neck carcinoma. Nucl Med Commun 2004;25:259-63
153. Kemerink GJ, Liem IH, Hofstra L, Boersma HH, Buijs WCAM, Reutelingsperger CPM, Heidendal GAK. Patient dosimetry of intravenously administered ^{99m}Tc-Annexin. J Nucl Med 2001;42:382–7
154. Goedemans WT, Panck KJ. A new simple method for labeling of proteins with ^{99m}Tc [abstract]. J Nucl Med Allied Sci 1989;33(3):286
155. Dumont EAW, Hofstra L, Van Heerde WL, et al. Cardiomyocyte death induced by myocardial ischemia and reperfusion: measurement with recombinant human annexin V in a mouse model. Circulation 2000;102:1564–8
156. Vanderheyden JL, Liu G, He J, Patel B, Hnatowich DJ. A comparison in normal mice of annexin V radiolabeled with ^{99m}Tc via hynic/tricine and MAG_3 [abstract]. J Nucl Med 2003;44(5):311P
157. McQuade P, Jones LA, Vanderheyden JL, Welch MJ. ^{94m}Tc and ^{64}Cu labeled annexin-V, positron emitting radiopharmaceuticals to study apoptosis [abstract]. J Labelled Cpd Radiopharm 2003;46(Suppl 1):S335
158. Decristoforo C, Mather SJ. The influence of chelator on the pharmacokinetics of ^{99m}Tc-labelled peptides. Q J Nucl Med 2002;46:195–205
159. Verbeke KA, Kieffer D, Vanderheyden JL, Steinmetz N, Green A, Verbruggen A. Influence of the co-ligand on the labelling and biodistribution of Tc-99m labelled Hynic-Annexin V [abstract]. Eur J Nucl Med Mol Imaging 2002;29(Suppl 1):S369
160. Verbeke K, Kieffer D, Vanderheyden JL, et al. Optimization of the preparation of ^{99m}Tc-labeled Hynic-derivatized Annexin V for human use. Nucl Med Biol 2003;30:771–8
161. Yang DJ, Kim EE. Imaging of apoptosis and hypoxia. In: Kim EE, Yang DJ, editors. Targeted molecular imaging in oncology. New York: Springer-Verlag; 2001. p. 215–28
162. Yang DJ, Azhdarinia A, Wu P. In vivo and in vitro measurement of apoptosis in breast cancer cells using ^{99m}Tc-EC-annexin V. Cancer Biother Radiopharm 2001;16:73–83
163. Kim EE, Yang DJ, Azhdarinia A, et al. Assessment of tumor growth using angiogenic and apoptotic agents [abstract]. Eur J Nucl Med Mol Imaging 2003;30(Suppl 2):S316

164. Umezawa K, Nakazawa K Uchihata Y, Otsuka M. Screening for inducers of apoptosis in apoptosis-resistant human carcinoma cells. Adv Enzyme Regul 1999;39:145–56
165. Lennon SV, Martin SJ, Cotter TG. Dose-dependent induction of apoptosis in human tumour cell lines by widely diverging stimuli. Cell Prolif 1991;24:203–14
166. Haberkorn U, Bellemann ME, Brix G, et al. Apoptosis and changes in glucose transport early after treatment of Morris hepatoma with gemcitabine. Eur J Nucl Med 2001;28:418–25
167. Zhu L, Liu BL, Guo YZ. Tc-99m direct labeling of annexin V for potential apoptosis imaging in vivo [abstract]. J Labelled Cpd Radiopharm 2003;46(Suppl 1):S324
168. Garron JY, Pasqualini R, Saccavini JC. Radiomarquage des anticorps monoclonaux er des peptides par le technetium 99m–voie directe. In: Comet M, Vidal M, editors. Radiopharmaceutiques: chimie des radiotraceurs et applications biologiques. Grenoble: Universitaires de Grenoble; 1998: 365–78
169. Subbarayan M, Häfeli UO, Feyes DK, Unnithan J, Emancipator SN, Mukhtar H. A simplified method for preparation of ^{99m}Tc-annexin V and its biologic evaluation for in vivo imaging of apoptosis after photodynamic therapy. J Nucl Med 2003;44:650–6
170. Reutelingsperger CPM, Hornstra G, Hemker HC. Isolation and partial purification of a novel anticoagulant from arteries of human umbilical cord. Eur J Biochem 1985; 151:625–9
171. Subbarayan M, Hafeli U, Mukhtar H. Cellular imaging of apoptosis induced by photodynamic therapy (PDT) using Tc-99m-Annexin V made by a novel method [abstract]. Mol Imaging Biol 2002;4(4 Suppl 1);S41
172. Huber R, Schneider M, Mayr I, Romisch J, Paques EP. The calcium binding sites in human annexin V by crystal structure analysis at 2.0 Angström resolution. Implications for membrane binding and calcium channel activity. FEBS Lett 1990;275:15–21
173. Tait JF, Smith C. Site-specific mutagenesis of annexin V: role of residues from Arg-200 to Lys-207 in phospholipid binding. Arch Biochem Biophys 1991;288:141–4
174. Mira J-P, Dubois T, Oudinet J-P, Lukowski S, Russo-Marie F, Geny B. Inhibition of cytosolic phospholipase A_2 by annexin V in differentiated permeabilized HL-60 cells. J Biol Chem 1997;272:10474–82
175. Montaville P, Neumann J-M, Russo-Marie F, Ochsenbein F, Sanson A. A new consensus sequence for phosphatidylserine recognition by annexins. J Biol Chem 2002;277:24684–93
176. Meers P. Location of tryptophans in membrane-bound annexins. Biochemistry 1990;29:3325–30
177. Meers P, Mealy T. Phospholipid determinants for annexin V binding sites and the role of tryptophan 187. Biochemistry 1994;33:5829–37
178. Dubois T, Mira J-P, Feliers D, Solito E, Russo-Marie F, Oudinet J-P. Annexin V inhibits protein kinase C activity via a mechanism of phospholipid sequestration. Biochem J 1998;330:1277–82
179. Tait JF, Brown DS, Gibson DF, Blankenberg FG, Strauss HW. Development and characterization of annexin V mutants with endogenous chelation sites for ^{99m}Tc. Bioconjug Chem 2000;11:918–25
180. Mariani G, Erba P, Pellegrino D, et al. Biodistribution patterns of native and mutant ^{99m}Tc-labeled annexin V in mice [abstract]. Cancer Biother Radiopharm 2003;18(2):290
181. Mariani G, Pellegrina D, Freer G, et al. Biodistribution of native and mutant annexin V in mice [abstract]. J Nucl Med 2002;43(5):138P
182. Mariani G, Pellegrino D, Freer G, Volterrani D, Bevilacqua G, Blankenberg F, Tait J, Strauss HW. Biodistribution patterns of native and mutant ^{99m}Tc-labeled annexin V in mice [abstract]. J Nucl Med 2003;44(5):153P–4P
183. Kuge Y, Sato M, Zhao S, et al. Does previous treatment with annexin V affect ^{99m}Tc-annexin V accumulation in the tumor before or after chemotherapy [abstract]? J Nucl Med 2003;44(5):180P–1P
184. Mochizuki T, Kuge Y, Zhao S, et al. Detection of apoptotic tumor response in vivo after a single dose of chemotherapy with ^{99m}Tc-annexin V. J Nucl Med 2003;44:92–7
185. Tait JF, Smith C, Gibson DF. Development of annexin V mutants suitable for labeling with Tc(I)-carbonyl complex. Bioconjug Chem 2002;13:1119–23
186. Alberto R, Schibli R, Egli A, Schubiger AP. A novel organometallic aqua complex of technetium for the labelling of biomolecules: synthesis of $[^{99m}Tc(OH_2)_3(CO)_3]^+$ from $[^{99m}TcO_4]^-$ in aqueous solution and its reaction with a bifunctional ligand. J Am Chem Soc 1998;120: 7987–8
187. Han ES, Sato N, Wong KJ, Park LS, Yu S, Vanderheyden JL, Carrasquillo JA, Paik CH. Labeling annexin V with ^{99m}Tc-tricarbonyl PADA improved its organ clearance property [abstract]. J Nucl Med 2002;43(5):374P
188. Ohtsuki K, Akashi K, Aoka Y, Blankenberg FG, Kopiwoda S, Tait JF, Straus HW. Technetium-99m HYNIC-annexin V: a potential radiopharmaceutical for the in vivo detection of apoptosis. Eur J Nucl Med 1999;26:1251–8
189. Blankenberg FG, Katsikis PD, Tait JF, et al. Imaging of apoptosis (programmed cell death) with ^{99m}Tc annexin V. J Nucl Med 1999;40:184–91
190. He J, Liu C, Vanderheyden JL, Liu G, Rusckowski M, Hnatowich DJ. Radiolabeling morpholinos with ^{188}Re carbonyl provides improved in vitro and in vivo stability to re-oxidation. Nucl Med Commun 2004:in press
191. Chang SM, Lai PH, Cheng HW, Lo JM. ^{99m}Tc (I) tricarbonyl labeled hynic-annexin V as a potential apoptosis imaging agent [abstract]. J Nucl Med 2003;44(5):316P
192. Li C, Wen X, Wu Q, et al. Apoptosis induced by drug treatments correlates with uptake of ^{111}In-labeled PEGylated annexin V in MDA-MB468 tumors [abstract]. J Nucl Med 2002;43(5):41P–2P
193. Ito M, Tomiyoshi K, Takahashi N, et al. Development of a new ligand, ^{11}C-labeled annexin V, for PET imaging of apoptosis [abstract]. J Nucl Med 2002;43(5):362P
194. Smith-Jones PM, Afroze A, Zanzonico P, Tait J, Larson SM, Strauss HW. ^{68}Ga labelling of annexin-V: comparison to ^{99m}Tc-annexin-V and ^{67}Ga-annexin [abstract]. J Nucl Med 2003;44(5):49P–50P
195. Dollé F, Hinnen F, Lagnel B, Boisgard R, Sanson A, Russo-Marie F, Tavitian B. Radiosynthesis of a [^{18}F]fluoropyridine-based maleimide reagent for protein labelling [abstract]. J Labelled Cpd Radiopharm 2003;46:S15
196. Boisgard R, Blondel A, Dolle F, et al. A new ^{18}F tracer for apoptosis imaging in tumor bearing mice [abstract]. J Nucl Med 2003;44(5):49P
197. Boisgard R, Vuillemard C, Dollé F, et al. New ^{18}F and ^{99m}Tc radiopeptides for apoptosis imaging in tumour-bearing mice [abstract]. Cancer Biother Radiopharm 2003;18(2): 282

198. Boisgard R, Blondel A, Vuillemard C, et al. A new spect tracer for improved apoptosis imaging in tumor bearing mice [abstract]. J Nucl Med 2003;44(5):98P
199. Blondel A, Laurent D, Vuillemard C, et al. Apoptosis detection using a new tracer for SPECT and PET imaging [abstract]. Mol Imaging Biol 2003;5(3):170–1
200. Ran S, Thorpe PE. Phosphatidylserine is a marker of tumor vasculature and a potential target for cancer imaging and therapy. Int J Radiat Oncol Biol Phys 2002;54:1479–84
201. Hashizume DM, Baluk P, Morikawa S, et al. Openings between defective endothelial cells explain tumor vessel leakiness. Am J Pathol 2000;156:1363–80
202. Nakamura N, Kuragaki C, Shidara Y, Yamaji K, Wada Y. Antibody to annexin V has anti-phospholipid and lupus anticoagulant properties. Am J Hematol 1995;49:347–8
203. Nakamura N, Shidara Y, Kawaguchi N, Azuma C, Mitsuda N, Onishi S, Yamaji K, Wada Y. Lupus anticoagulant autoantibody induces apoptosis in umbilical vein endothelial cells: involvement of annexin V. Biochem Biophys Res Commun 1994;205:1488–93
204. Arai T, Matsubayashi AT, Sugi T, et al. Anti-annexin A5 antibodies in reproductive failures in relation to antiphospholipid antibodies and phosphatidylserine. Am J Reprod Immunol 2003;50:202–8
205. Rodriguez-Garcia MI, Fernandez JA, Rodriguez A, Fernandez MP, Gutierrez C, Torre-Alonso JC. Annexin V autoantibodies in rheumatoid arthritis. Ann Rheum Dis 1996;55:895–900
206. Kobayashi H, Kusakabe K Kanaya K, Momose M, Nagamatsu H, Okawa T, Kaneko N. Myocardial ischemia memory imaging: time course of In-111-DTPA anti-annexin V antibody uptake in the ischemic area [abstract]. J Nucl Med 1999;40(5 Suppl S):P818
207. Kobayashi H, Kaneko N, Kanaya K, Momose M, Kusakabe K, Okawa T, Kasanuki H. Myocardial ischemia memory imaging using monoclonal antibodies for myocardial annexin V [abstract]. Eur J Nucl Med 1999;26(9):OS341
208. Kobayashi H, Kaneko N, Kanaya K, Momose M, Kusakabe K, Okawa T, Sakomura Y, Horie T. Myocardial ischemia memory imaging using monoclonal antibodies for myocardial annexin V [abstract]. Circulation 1998;98(17 Suppl S):484
209. Benevolensky D, Belikova Y, Mohammadzadeh R, et al. Expression and localization of the annexins II, V, and VI in myocardium from patients with end-stage heart failure. Lab Invest 2000;80:123–33
210. Strauss HF, Narula J, Blankenberg F. Radioimaging to identify myocardial cell death and probably injury. Lancet 2000;356:180–1
211. Kaneko N, Matsuda R, Hosoda S, Kajita T, Ohta Y. Measurement of plasma annexin V by ELISA in the early detection of acute myocardial infarction. Clin Chim Acta 1996;251:65–80
212. Bleackley C, Heibein JA. Enzymatic control of apoptosis. Nat Prod Rep 2001;18:431–40
213. Talanian RV, Brady KD, Cryns VL. Caspases as targets for anti-inflammatory and anti-apoptotic drug discovery. J Med Chem 2000;43:1–21
214. Reed JC, Tomaselli KJ. Drug discovery opportunities from apoptosis research. Curr Opin Biotechnol 2000;11:586–92
215. Haberkorn U, Kinscherf R, Krammer PH, Mier W, Eisenhut M. Investigation of a potential scintigraphic marker of apoptosis: radioiodinated Z-Val-Ala-DL-Asp(*O*-methyl)-fluoromethylketone. Nucl Med Biol 2001;28:793–8
216. Fischer U, Jänicke RU, Schulze-Osthoff K. Many cuts to ruin: a comprehensive update of caspase substrates. Cell Death Differ 2003;10:76–100
217. Alauddin MM, Hu J, Prakash GKS, Conti PS, Olah GA. A general synthesis of [^{18}F]-labeled α-trifluoromethyl ketones for PET imaging [abstract]. J Labelled Cpd Radiopharm 2003;46:S189
218. Halestrap AP, Kerr PM, Javadov S, Woodfield K-Y. Elucidating the molecular mechanism of the permeability transition pore and its role in reperfusion injury of the heart. Biochim Biophys Acta 1998;1366:79–94
219. Zoratti M, Szabò I. The mitochondrial permeability transition. Biochim Biophys Acta 1995;1241:139–76
220. Zamzami N, Kroemer G. The mitochondrion in apoptosis: how Pandora's box opens. Nat Rev: Mol Cell Biol 2001;2:67–71
221. Halestrap A, McStay GP. Clarke SJ. The permeability transition pore complex: another view. Biochimie 2002;84:153–66
222. Hirsch T, Susin SA, Marzo I, Marchetti P, Zamzami N, Kroemer G. Mitochondrial permeability transition in apoptosis and necrosis. Cell Biol Toxicol 1998;14:141–5
223. Desagher S, Martinou J-C. Mitochondria as the central control point of apoptosis. Trends Cell Biol 2000;10:369–77
224. Decaudin D, Marzo I, Brenner C, Kroemer G. Mitochondria in chemotherapy-induced apoptosis: a prospective novel target of cancer therapy (review). Int J Oncol 1998;12:141–52
225. Bernardi P, Petronili V, Di Lisa F, Forte M. A mitochondrial perspective on cell death. Trends Biochem Sci 2001; 26:112–7
226. Madar I, Ravert HT, Nelkin B, Scheffel U, Hilton J, Dannals RF, Frost JJ. Physicochemical characteristics and uptake kinetics of voltage indicator [F-18] phosphonium cations [abstract]. J Nucl Med 2003;44(5):50P
227. Madar I, Ravert HT, Hilton J, Dannals RF, Frost JJ., Hare JM. Quantitative imaging of cardiomyopathy in heart failure using the voltage indicator [F-18]p-fluorobenzyl triphenylphosphonium ([F-18]p-FBnTP) and PET [abstract]. J Nucl Med 2003;44(5):87P
228. Madar I, Nelkin B, Isaacs JT, Ravert HT, Scheffel U, Dannals RF, Frost JJ. In vitro and in vivo correlation of taxotere-induced apoptosis in malignant cells and accumulation of the voltage indicator [F-18]p-fluorobenzyltriphenyl phosphonium ([F-18]p-FBnTP) [abstract]. J Nucl Med 2003;44(5):179P–80P
229. Madar I, Isaacs TD, Ravert HT, Scheffel U, Dalrymple S, Dannals RF, Frost JJ. Detection of androgen depletion-induced apoptosis in prostate using the voltage indicator [F-18]p-fluorobenzyltriphenyl phosphonium ([F-18]p-FBnTP), in vivo [abstract]. J Nucl Med 2003;44(5):180P
230. Kothan S, Vergote J, Dechsupa S, Mankhetorn S, Hauet N, Moretti JL. Influence of flavanoid on the mitochondrial membrane potential, on Pgp efflux assessed by ^{99m}Tc-MIBI and on apoptosis assessed by ^{99m}Tc-Annexin V in multidrug resistant and sensitive cells [abstract]. Eur J Nucl Med Mol Imaging 2003;30(Suppl 2):S316
231. Blankenberg FG, Storrs RW, Naumovski L, Goralski T, Spielman D. Detection of apoptotic cell death by proton nuclear magnetic resonance spectroscopy. Blood 1996; 88:1951–6
232. Brisdelli F, Iorio E, Knijn A, et al. Two-step formation of ^{1}H NMR visible mobile lipids during apoptosis of paclitaxel-treated K562 cells. Biochem Pharmacol 2003; 65:1271–80

233. Valonen P, Griffin J, Vaisanen T, et al. Macromolecular and lipid resonances in apoptosing BT4C glioma cells in vitro and tumors in vivo [abstract]. Proc Int Soc Magn Reson Med 2002;10:26
234. Goldberg A, Poptani H, Duvvure U, Wherli S, Leigh J, Glickson J, Delikatny E. Quantification of unsaturated lipid changes in cyclophosphamide treated tumors [abstract]. Proc Int Soc Magn Reson Med 2002;10:2145
235. Blankenberg FG, Katsikis PD, Storrs RW, Beaulieu C, Spielman D, Chen JY, Naumovski L, Tait JF. Quantitative analysis of apoptotic cell death using proton nuclear magnetic resonance spectroscopy. Blood 1997;89:3778–86
236. Locke S, Brauer M. Response of the rat liver in situ to bromobenzene: in vivo proton MRI an ^{31}P MRS studies. Toxicol Appl Pharmacol 1991;110:416–28
237. Henke J, Flogel U, Pfeuffer J, Leibfritz D. Multinuclear NMR studies of apoptotic changes in a human tumor cell line during miltefosin treatment [abstract]. Proc Int Soc Magn Reson Med 1999;7:1343
238. Hakumaki JM, Poptani H, Sandmair AM, Ylä-Herttuala S, Kauppinen RA. ^{1}H MRS detects polyunsaturated fatty acid accumulation during gene therapy of glioma: implications for the in vivo detection of apoptosis. Nat Med 1999;5:1323–7
239. Brauer M. In vivo monitoring of apoptosis. Prog Neuropsychopharmacol Biol Psychiatry 2003;27:323–31
240. Poptani H, Puumalainen AM, Grohn O, Loimas S, Kainulainen R, Kauppinen RA. Monitoring thymidine kinase and ganciclovir-induced changes in rat malignant gliomas in vivo by MRI. Cancer Gene Ther 1998;5:101–9
241. Zhao M, Pipe J, Bonnett J, Evelhoch J. Early detection of treatment response by diffusion-weighted ^{1}H NMR spectroscopy in a murine tumour in vivo. Br J Cancer 1996;73:61–4
242. Davletov BA, Sudhof TC. A single C_2 domain from synaptotagmin I is sufficient for high affinity Ca^{2+}/phospholipid binding. J Biol Chem 1993;26:26386–90
243. Sutton BR, Davletov BA, Berghuis AM, Südhof TC, Sprang SR. Structure of the first C_2 domain of synaptotagmin I: a novel Ca^{2+}/phospholipid-binding fold. Cell 1995;80:929–38
244. Zhao M, Beauregard DA, Loizou L. Non-invasive detection of apoptosis using magnetic resonance imaging and a targeted contrast agent. Nat Med 2001;7:1241–3
245. Schellenberger EA, Bogdanov A, Högemann D, Weissleder R, Josephson L, Tait J. Annexin V-CLIO: a nanoparticle for detecting apoptosis by MRI. Mol Imaging 2002;1:1–6
246. Giorgetti AA, Pingitore A, Di Quirico S, Landi P, Lombardi M., Marzullo P. Non-invasive quantitative assessment of transmural extent of myocardial necrosis by means of contrast-enhanced magnetic resonance:comparison with post-nitrate ^{99m}Tc-tetrofosmin GSPECT [abstract]. J Nucl Cardiol 2003;10(1):S64
247. Pan D, Sun H, Rich TA, Berr SS. Evaluation of mouse tumor response to radiation therapy by near infrared fluorescence imaging using cyanine 5.5-Annexin V [abstract]. Mol Imaging Biol 2003;5(3):162
248. Mandl SJ, Mari C, Contag CH, Tait JF, Blankenberg FG. Increased annexin V uptake precedes tumor cell loss in mice with luciferase expressing BCL-1 lymphoma [abstract]. J Nucl Med 2003;44(5):179P
249. Hartung D, Petrov A, Kolodgie F, et al. Preventing apoptosis should constitute the basis of management of atherosclerosis: pan-caspase inhibitor simulate the effects of diet withdrawal and statin therapy [abstract]. J Nucl Med 2003;44(5):1P
250. Mari C, Yenari M, Tait JF, Zhu JH, Goris ML, Blankenberg FG. Application of dedicated small animal SPECT: radiolabeled annexin V tomographic imaging of ischemic reperfusion injury in the rat brain [abstract]. J Nucl Med 2003; 44(5):215P
251. Dumont EA, Petrov A, Narula N, Haider N, Reutelingsperger CPM, Narula J, Hofstra L. Tc-99m Annexin-V imaging non-invasively detects ischemic memory as prolonged but reversible sarcolemmal phosphatidyl serine expression occurs in myocardial ischemia [abstract]. J Nucl Med 2003;44(5):104P
252. Van den Eijnde SM, Boshart L, Reutelingsperger CPM, De Zeeuw CI, Vermeij-Keers C. Phosphatidylserine plasma membrane asymmetry in vivo: a pancellular phenomenon which alters during apoptosis. Cell Death Differ 1997; 4:311–6
253. Sweeney TJ. Visualizing the kinetics of tumor-cell clearance in living animals. Proc Natl Acad Sci USA 1999;96:12044–9
254. Reynolds JS, Troy TL, Mayer RH, et al. Imaging of spontaneous canine mammary tumors using fluorescent contrast agents. Photochem Photobiol 1999;70:87–94
255. Dumont EA, Reutelingsperger CPM, Smits JFM, et al. Real-time imaging of apoptotic cell-membrane changes at the single cell level in the beating murine heart. Nat Med 2001;7:1352–5
256. Czarnota GJ, Kolios MC, Vaziri H, Benchimol S, Ottensmeyer FP, Sherar MD, Hunt JW. Ultrasonic biomicroscopy of viable, dead and apoptotic cells. Ultrasound Med Biol 1997;23:961–5
257. Czarnota GJ, Kolios MC, Abraham J, et al. Ultrasound imaging of apoptosis: high-resolution non-invasive monitoring of programmed cell death in vitro, in situ and in vivo. Br J Cancer 1999;81:520–7
258. Makin G, Hickman JA. Apoptosis and cancer chemotherapy. Cell Tissue Res 2000;301:143–52
259. Roman S, Petrusca D, Moldovan I, Paraoan M, Petrescu A, Damian D, Noica N, Sulica A. Evaluation of apoptosis of tumor and of apparently normal cells in human renal carcinoma. Immunol Lett 1999;67:15–22
260. Renehan AG, Bach SP, Potten CS. The relevance of apoptosis for cellular homeostasis and tumorigenesis in the intestine. Can J Gastroenterol 2001;15:166–76
261. Sheridan MT, Cooper RA, West CML. A high ratio of apoptosis to proliferation correlates with improved survival after radiotherapy for cervical adenocarcinoma. Int J Radiat Oncol Biol Phys 1999;44:507–12
262. Dowsett M, Archer C, Assersohn L, et al. Clinical studies of apoptosis and proliferation in breast cancer. Endocr Relat Cancer 1999;6:25–8
263. Yaoita H, Ogawa K, Maehara K, Maruyama Y. Apoptosis in relevant clinical situations: contribution of apoptosis in myocardial infarction. Cardiovasc Res 2000;45:630–41
264. Arola OJ, Saraste A, Pulkki K, Kallajoki M, Parvinen M, Voipio-Pulkki L-M. Acute doxorubicin cardiotoxicity involves cardiomyocyte apotosis. J Cancer Res 2000; 60:1789–92
265. Diwakar J. Cardiotoxicity of doxorubicin and other anthracycline derivatives. J Nucl Cardiol 2000;7:53–62
266. Nakamura T, Ueda Y, Juan Y, Katsuda S, Takahashi H, Koh E. Fas-mediated apoptosis in adriamycin-induced cardiomyopathy in rats. Circulation 2000;102:572–8
267. Sandri M, Carraro U. Apoptosis of skeletal muscles during development and disease. Int J Biochem Cell Biol 1999; 31:1373–90

268. Narula J, Arbustini B, Chandrashekhar Y, Schwaiger M. Apoptosis and the systolic dysfunction in congestive heart failure. Cardiol Clin 2001;19:113–26
269. Haunstetter A, Izumo S. Future perspectives and potential implications of cardiac myocyte apoptosis. Cardiovasc Res 2000;45:795–801
270. Kockx MM, Herman AG. Apoptosis in atherosclerosis: beneficial or detrimental? Cardiovasc Res 2002;45:736–46
271. Rössig L, Dimmeler S, Zeiher AM. Apoptosis in the vascular wall and atherosclerosis. Basic Res Cardiol 2001; 96:11–22
272. McCarthy NJ, Bennett MR. The regulation of vascular smooth muscle cell apoptosis. Cardiovasc Res 2000; 45:747–55
273. Sabbah HN. Apoptotic cell death in heart failure. Cardiovasc Res 2000;45:704–12
274. Haunstetter A, Izumo S. Basic mechanisms and implications for cardiovascular disease. Circ Res 1998;82:1111–29
275. Elsässer A, Suzuki K, Lorenz-Meyer S, Bode C, Schaper J. The role of apoptosis in myocardial ischemia: a critical appraisal. Basic Res Cardiol 2001;96:219–26
276. Zhao Z-Q, Nakamura M, Wang N-P, et al. Reperfusion induces myocardial apoptotic cell death. Cardiovasc Res 2000;45:651–60
277. Ogura Y, Krams SM, Martinez OM, et al. Radiolabeled annexin V imaging: diagnosis of allograft rejection in an experimental rodent model of liver transplantation. Radiology 2000;214:795–800
278. Blankenberg FG, Robbins RC, Stoot JH, Vriens PW, Berry GJ, Tait JF, Strauss HW. Radionuclide imaging of acute lung transplant rejection with annexin V. Chest 2000;117:834–40
279. Blankenberg FG, Strauss HW. Non-invasive diagnosis of acute heart- or lung transplant rejection using radiolabeled annexin V. Pediatr Radiol 1999;29:299–305
280. Puig M, Ballester M, Matías-Guiu X, et al. Burden of myocardial damage in cardiac allograft rejection: scintigraphic evidence of myocardial injury and histologic evidence of myocyte necrosis and apoptosis. J Nucl Cardiol 2000; 7:132–9
281. Skulachev VP. Phenoptosis: programmed cell death of an organism. Biochemistry 1999;64:1418–26
282. Charriaut-Marlangue C, Remolleau S, Aggoun-Zounaoui D, Ben-Ari Y. Apoptosis and programmed cell death: a role in cerebral ischemia. Biomed Pharmacother 1998;52:264–9
283. Li Y, Powers C, Jiang N, Chopp M. Intact, injured necrotic and apoptotic cells after focal cerebral ischemia in the rat. J Neurol Sci 1998;156:119–32
284. Raina AK, Hochman A, Zhu X, et al. Abortive apoptosis in Alzheimer's disease. Acta Neuropathol 2001;101:305–10
285. Mattson MP. Apoptosis in neurodegenerative disorders. Nat Rev: Mol Cell Biol 2000;1:120–30
286. Martin LJ. Neuronal cell death in nervous system development, disease, and injury (review). Int J Mol Med 2001; 7:455–78
287. Rand JH. The annexinopathies: a new category of diseases. Biochim Biophys Acta 2000;1498:169–73
288. Grodzicky T, Elkon KB. Apoptosis in rheumatic diseases. Am J Med 2000;108:73–82
289. Vannier MW. Imaging apoptosis in rheumatoid arthritis. J Nucl Med 2002;43:1366–7
290. Andrade F, Casciola-Rosen L, Rosen A. Apoptosis in systemic lupus erythematosus: clinical implications. Rheum Dis Clin North Am 2000;26:215–27
291. Bastian BC. Annexins in cancer and autoimmune diseases. Cell Mol Life Sci 1997;53:554–36
292. Ueda N, Kaushal GP, Shah SV. Apoptotic mechanisms in acute renal failure. Am J Med 2000;108:403–15
293. Ortiz A, Cuadrado SG, Lorz C, Egido J. Apoptosis in renal diseases. Front Biosci 1996;1:30–47
294. Ramakers B, Oyen WJ, Smits P, Rongen GA. Tc-99m-Hynic-Annexin V in a human model for ischemic preconditioning [abstract]. J Nucl Med 2003;44(5):194P
295. Del Vecchio S, Zannetti A, Ciarmiello A, et al. Dynamic coupling of ^{99m}Tc-MIBI efflux and apoptotic pathway activation in untreated breast cancer patients. Eur J Nucl Med Mol Imaging 2002;29:809–14
296. Thimister PW, Hofstra L, Liem IH, et al. In vivo detection of cell death in the area at risk in acute myocardial infarction. J Nucl Med 2003;44:391–6